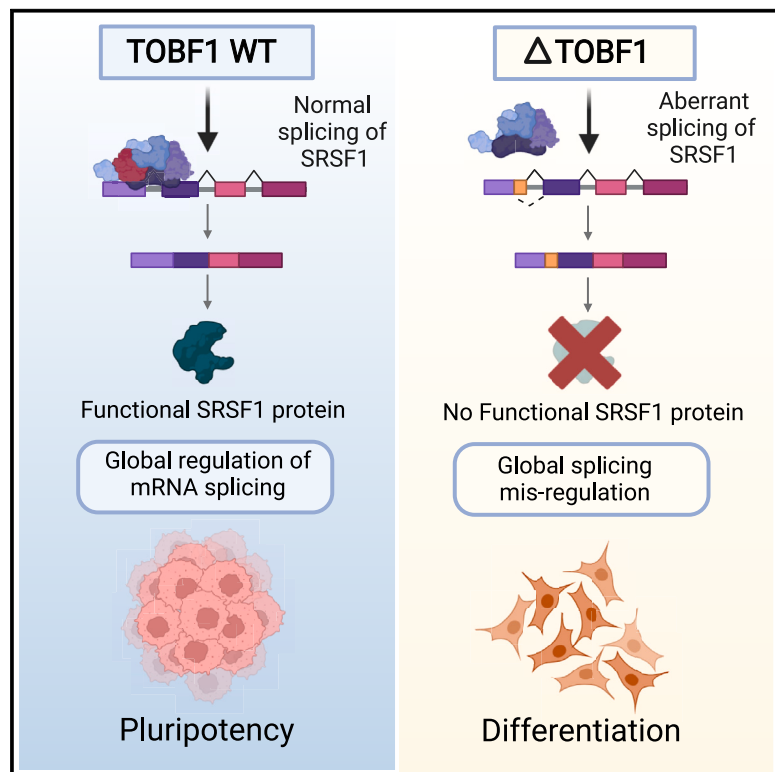


TOBF1 modulates mouse embryonic stem cell fate through regulating alternative splicing of pluripotency genes

Graphical abstract



Authors

Meghali Aich, Asgar Hussain Ansari, Li Ding, ..., Souvik Maiti, Frank Buchholz, Debojyoti Chakraborty

Correspondence

debojyoti.chakraborty@igib.in

In brief

Aich et al. elucidate the role of a previously uncharacterized protein, TOBF1, in the stabilization of mouse embryonic pluripotency. Their study reveals that TOBF1 regulates the alternative splicing of multiple pluripotency regulatory transcripts through cotranscriptional splicing in discrete nuclear foci in ESCs.

Highlights

- TOBF1 maintains mouse ESC identity through regulation of alternate splicing
- This happens cotranscriptionally in discrete nuclear foci and impacts multiple genes
- Among them, alternate isoform usage of SRSF1 leads to global splicing changes
- Loss and gain of TOBF1 lead to concomitant changes in the levels of pluripotency genes



Article

TOBF1 modulates mouse embryonic stem cell fate through regulating alternative splicing of pluripotency genes

Meghali Aich,^{1,2} Asgar Hussain Ansari,^{1,2} Li Ding,³ Vytautas Iesmantavicius,⁴ Deepanjan Paul,¹ Chunaram Choudhary,⁴ Souvik Maiti,^{1,2} Frank Buchholz,³ and Debojyoti Chakraborty^{1,2,5,*}

¹CSIR- Institute of Genomics and Integrative Biology, New Delhi 110025, India

²Academy of Scientific and Innovative Research (AcSIR), Ghaziabad 201002, India

³Medical Systems Biology, UCC, Medical Faculty Carl Gustav Carus, TU Dresden, Fetscherstrasse 74, 01307 Dresden, Germany

⁴The Novo Nordisk Foundation Center for Protein Research, University of Copenhagen, Copenhagen, Denmark

⁵Lead contact

*Correspondence: debojyoti.chakraborty@igib.in

<https://doi.org/10.1016/j.celrep.2023.113177>

SUMMARY

Embryonic stem cells (ESCs) can undergo lineage-specific differentiation, giving rise to different cell types that constitute an organism. Although roles of transcription factors and chromatin modifiers in these cells have been described, how the alternative splicing (AS) machinery regulates their expression has not been sufficiently explored. Here, we show that the long non-coding RNA (lncRNA)-associated protein TOBF1 modulates the AS of transcripts necessary for maintaining stem cell identity in mouse ESCs. Among the genes affected is serine/arginine splicing factor 1 (SRSF1), whose AS leads to global changes in splicing and expression of a large number of downstream genes involved in the maintenance of ESC pluripotency. By overlaying information derived from TOBF1 chromatin occupancy, the distribution of its pluripotency-associated OCT-SOX binding motifs, and transcripts undergoing differential expression and AS upon its knockout, we describe local nuclear territories where these distinct events converge. Collectively, these contribute to the maintenance of mouse ESC identity.

INTRODUCTION

Mouse embryonic stem cells (mESCs) are derived from the inner cell mass of a developing blastocyst and are ex vivo equivalent to the epiblast lineage, thus sharing the same developmental potential. These cells are characterized by their ability for a high capacity of *in vitro* self-renewal and the conservation of developmental pluripotency to differentiate into any of the three embryonic lineages, ectoderm, endoderm, and mesoderm.^{1–3} As such, mESCs possess clinical potential for cell-based therapy and regenerative medicine research.⁴ To harness the quality and applicability of mESCs, it is important to understand the fundamental properties and molecular mechanisms that govern this identity.

Various studies have established the role of POU5F1, SOX2, NANOG, KLF4, and ESRRB as the core transcription factors that regulate the pluripotency network of mESCs.^{5–7} Pluripotent cells have distinct chromatin structures enriched for active histone marks and hyperdynamic binding of structural proteins.⁸ They also have global hyperactive transcriptional states and enhanced chromatin modifiers as compared with differentiated cells.^{9,10} The interplay between the pluripotency network and external cues orchestrates the *in vivo* self-renewal and undifferentiated stem cell state. These concepts have emerged from

genetic, biochemical, and molecular studies of transcription factors, chromatin regulators, non-coding RNAs, mRNA splicing, and translational control.^{11–13}

In pluripotent cells, RNA-binding proteins (RBPs) are part of the extended regulatory network that dynamically dictates the establishment of a stem cell-like state or induction of differentiation. Among the first RBPs, Lin28 proteins were recognized as regulators of pluripotency and stem cell maintenance.¹⁴ At various levels of post-transcriptional control, RBPs influence the stem cell state including RNA modification (METTL3/14, ADAR), alternative polyadenylation (FIP1), alternative splicing (AS) (RBFOX2, SON), nuclear export (THOC2/5), RNA stability (TRIM71, ZFP36L1, PUM1), and translation (ESRP1, L1TD1).^{15–17}

AS is a distinct event in metazoan genomes by which different combinations of exonic splice sites in pre-mRNA are selected to generate varied structural and functional mRNA and protein molecules.^{18–20} DNA binding and transcription factors also multitask at the level of RNA to regulate AS. For example, NACC1 regulates the expression of other splicing factors such as MBNL1 and RBFOX1, which indirectly controls the ESC-specific AS events to maintain the stem cell behavior.²¹ Depletion of the spliceosome-associated factor SON leads to loss of pluripotency and cell death due to mis-splicing of the key pluripotency factors



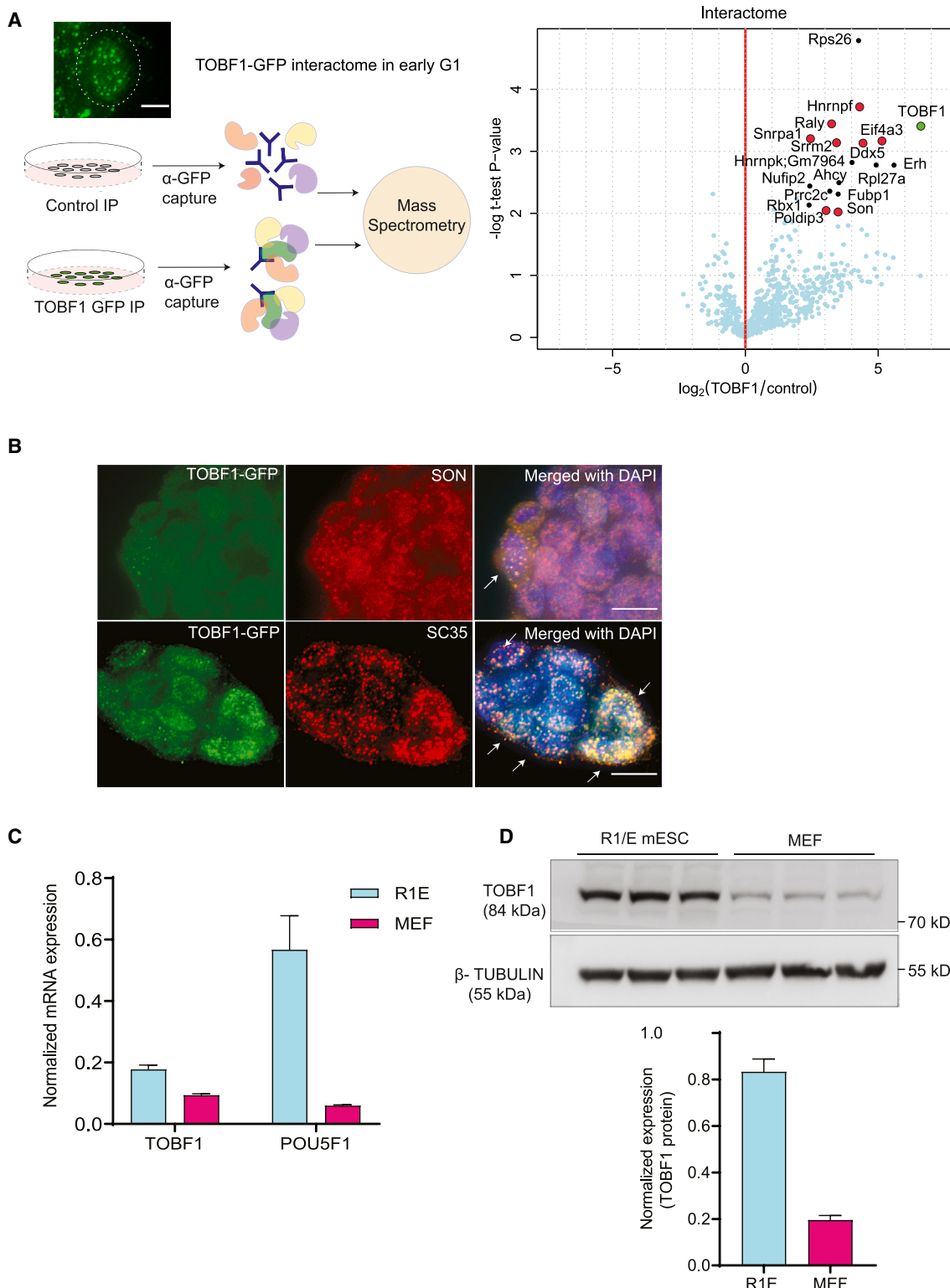


Figure 1. TOBF1 interactome in early G1 phase shows enrichment of splicing regulators

(A) Schematic showing TOBF1-GFP BAC-tagged cells form bright puncta in specific cell-cycle phase. Scale bar: 5 μm. TOBF1-GFP in tagged cells is immunoprecipitated with anti-GFP antibody (control, R1/E mESCs) in the G1 phase through Demecolcine treatment and release (STAR Methods). Mass spectrometry

(legend continued on next page)

OCT4, PRDM14, and MED24.²² Other splicing factors including RBM9, ESRP1, SFRS2, MBNL1/2, and HNRNPLL play specific roles in regulating pluripotency by stimulating the precise splicing of various transcripts, thereby altering global transcriptome expression.^{23–26} Another splicing factor, hnRNP K, mediating proliferation and maintenance of myoblasts, profoundly affects the cell-cycle patterns, thus indicating an initiation of differentiation.²⁷ Among others, serine/arginine splicing factor 1 (SRSF1) has been shown to affect splicing patterns of genes implicated in both embryonic and adult stem cells and has shown characteristics of a protooncogene as well.^{28–30}

Studies have shown the role of microRNAs and long non-coding RNAs in transcriptional regulation and post-transcriptional monitoring roles to support the self-renewal and pluripotency in ESCs^{31,32}. Advances in high-throughput cross-linking and immunoprecipitation followed by sequencing (CLIP-seq) and genome association studies have revealed that long non-coding RNAs (lncRNAs) bind with one or more RBPs and coordinately regulate gene expression.^{33,34} In one study, it was seen that close to 75% of 226 lncRNAs expressed in mESCs have binding sites for at least 1 of 9 pluripotency-associated transcription factors (OCT4, SOX2, NANOG, c-MYC, n-MYC, KLF4, ZFX, SMAD, and TCF3), and upon knockdown of 11 pluripotency-associated transcription factors, 60% mESC-expressed lncRNAs showed significant downregulation.³⁵

Previously, through a genome-wide endoribonuclease-prepared small interfering RNA (esiRNA) screen study, we had identified 594 lncRNA targets for loss of function in mouse cells, of which lncRNA *Panct1* was molecularly characterized to have a positive role in maintaining the ESC identity.³⁶ A subsequent report revealed that the lncRNA *Panct1* interacts with an X chromosome-associated protein TOBF1 (A830080D01Rik/BCLAF3) and transiently localizes to genomic loci containing the OCT-SOX motif in a specific cell-cycle-regulated manner. This RNA-protein association is indispensable for maintaining the mESC state.³⁷ Interestingly, in a recent study using a genome-scale CRISPR screen, knockout (KO) of TOBF1 (also called BCLAF3) was revealed to support the Wnt-independent self-renewal of gastric epithelial cells in mouse gastric epithelial organoid models.³⁸ This suggests that TOBF1 might have distinct roles dependent on the individual cell type and/or the tissue of expression.

TOBF1 in mice is derived from X chromosome and belongs to the BCLAF1/THRAP3 family of proteins and is also known as BCLAF1 and THRAP3 family member 3 (BCLAF3; UniProt: A2AG58). THRAP3 in humans is a spliceosome component and a subunit of the TRAP complex that has been reported to play a role in mRNA decay and pre-mRNA splicing.³⁹ BCLAF1 and THRAP3 are RNA processing factors that have a role in

DNA damage response pathway and genomic stability and prevention of oncogenic transformation.^{40,41} Except for its role in self-renewal of gastric epithelial cells in mice,³⁸ TOBF1's role has remained largely uncharacterized, particularly in ESCs.

RESULTS

TOBF1 interactome shows enrichment of splicing regulators

Our earlier studies on TOBF1 clearly demonstrated distinct hallmarks of its cellular localization: bright puncta in early G1 phase of the cell cycle coupled with an association with chromatin. Notably, these were sites where the lncRNA *Panct1* localized as well and marked transient yet defined territories of unknown function.³⁷ To precisely pinpoint the mode of action of TOBF1 in this phase, we first performed an affinity purification followed by mass spectrometry-based identification of the associated proteins upon TOBF1 pull-down from a BAC-tagged TOBF1-GFP mESC line ([STAR Methods](#)). A total of 672 proteins were pulled down, and the bait (TOBF1-GFP) showed the highest enrichment (>20 peptides per replicate) as expected. In order to identify the potential interactors of TOBF1, we set up a stringent cutoff ($-\log p$ value > 2) and further shortlisted potential interactors based on their presence in at least 2 out of 3 control pull-downs. Finally, we identified 17 proteins with high confidence that were significantly enriched in the TOBF1-GFP pull-down samples and not detected in controls ([Figure 1A](#); [Table S1](#)).

Pathway analysis showed that 8 of the 17 proteins (47%) had roles in the processing and splicing of transcript isoforms ([Table S1](#)). Some of these are well-characterized regulators of specific mRNA processing, including SON, EIF4A3, SRRM2, ERH, RALY, hnRNP-F, etc.^{42–45} ([Figures 1A](#) and [S1A](#)). In addition, the interactome profile revealed ribosomal and ribonucleoproteins such as RPL27A, RPS26, and hnRNP-K that have been reported to affect the complex ribosomal biogenesis and mRNA stability pattern in the ESC condition.^{46–48} ([Figure S1A](#)). Taken together, these results suggest that TOBF1 might be involved in the regulation of mRNA processing in mESCs.

Among the top TOBF1-interacting proteins, the presence of SON was particularly interesting since it has been implicated in the regulation of proper splicing of mRNA transcripts encoding pluripotency regulators in human ESCs.²² In a subsequent study, SON was shown to associate with BCLAF1 and THRAP3,⁴⁹ both of which belong to the same family as mouse TOBF1. Coimmunofluorescence (coIF) revealed that TOBF1 and SON colocalized (Pearson's colocalization coefficient of ~0.7) in discrete puncta in ESC nucleus ([Figure 1B](#)). Importantly, TOBF1 also showed

interactome profile showing interaction between TOBF1 and different mRNA processing and splicing proteins, a few of which are specific to stem cells (marked in red) with fold change (\log_2) ≥ 2 and p value < 0.05 .

(B) Representative coimmunofluorescence (coIF) images of combined TOBF1 (green) and SON (red) (top) and TOBF1 (green) and SC35 (red) (bottom), showing colocalization of TOBF1-SON and TOBF1-SC35 colocalization in TOBF1-GFP cells. Arrows mark colocalized spots. DNA is counterstained with DAPI and represented in blue. Scale bar: 10 μ m.

(C) qRT-PCR showing the steady-state mRNA levels of *Tobf1* and *Pouf5f1* in R1E WT mESCs and MEFs, normalized with β -actin. Error bars indicate the SD of three independent replicates.

(D) Western blot showing expression of TOBF1 in R1E WT mESCs and MEFs as ~84 kDa protein. β -Tubulin taken as loading control. Bar plot with error bars showing SD of the quantification of the western blot with three independent replicates.

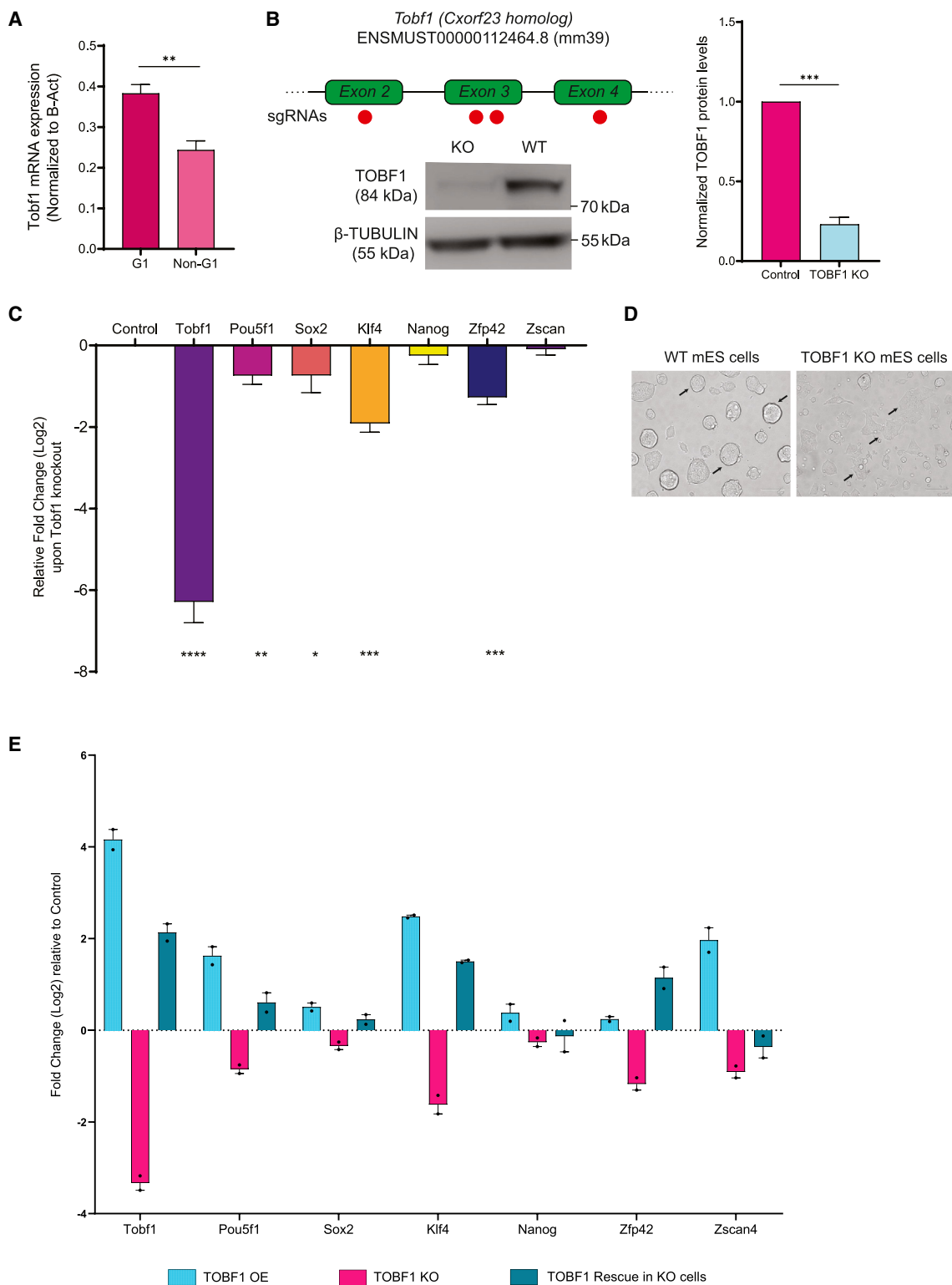


Figure 2. TOBF1 KO leads to loss of ESC identity

(A) Bar plot showing absolute steady-state mRNA levels of *Tobf1* in G1 and non-G1 sorted cells using ES-FUCCI system. *Tobf1* values are normalized with β -actin. Error bars indicate the SD of three independent replicates. *p < 0.05, **p < 0.001, ***p < 0.0001 (Student's t test).

(legend continued on next page)

colocalization with another canonical nuclear speckle marker and splicing regulator, SC-35⁵⁰ (Figure 1B), suggesting that the bright puncta in early G1 phase correspond to nuclear speckles (Pearson's colocalization coefficient of ~0.75), potentially signifying a focal point for TOBF1's RNA processing role.

Next, we performed coimmunoprecipitation of SON and TOBF1 and found that these proteins physically interact in mESCs (Figure S1B). It is well known that mRNA processing and splicing factors often localize to the nuclear speckles (NSs),⁵¹ and NSs are the hub for various mRNA post-transcriptional modifications. To validate that the TOBF1 interaction was specific to splicing-associated factors present in NSs, we probed another spliceosome-associated protein, RPS26, and found that TOBF1 physically associates with it (Figure S1B). These results establish that TOBF1 is indeed a bona fide member of the spliceosome-associated proteome in the early G1 phase of the cell cycle in mESCs and that the distinct TOBF1 puncta observed in the early G1 phase correlate with NSs.

To ensure that the BAC-tagged TOBF1-GFP cell line retains the cytoarchitecture of the endogenous TOBF1 protein, we also validated the above observations with a commercially available TOBF1 antibody. We found that the TOBF1-GFP signal completely colocalized with the TOBF1 antibody signal (Figure S1C). Importantly, in an untagged cell line (R1/E wild-type [WT] cells) too, the TOBF1 antibody displayed a mixture of bright puncta and diffused signal patterns as seen in the BAC-tagged cells (Figure S1D). Together, these data show that the TOBF1-GFP BAC-tagged signal is a bona fide representation of the TOBF1 localization pattern in mESCs.

High TOBF1 expression is a hallmark of mESC pluripotency

Pluripotent cells have a complex regulatory network that distinctly differs from differentiated cells. The set of proteins required for the maintenance of an ESC state are specific in their expression and function, and as cells undergo differentiation, they are replaced by others.^{52,53} Because esiRNA-mediated transient knockdown of TOBF1 had previously shown a reduction in *Pou5f1* and *Klf4* mRNA levels,³⁷ both of which are signatures of pluripotent mESCs, we investigated if elevated expression of TOBF1 is a marker of undifferentiated stem cells. To this end, we checked the expression of TOBF1 in R1E pluripotent mESCs and compared with a mouse embryonic fibroblast (MEF) line that is differentiated and does not show pluripotent characteristics. We observed that both at the level of mRNA and protein, TOBF1 expression in mESCs was higher (~2-fold at mRNA and ~4-fold at protein levels) than MEF cells, suggest-

ing that as cells exit from pluripotency, TOBF1 levels decline (Figures 1C and 1D). Next, we investigated the heterogeneity in TOBF1 levels across a small subset of mouse tissues and cell lines (liver, kidney, lung, heart, prefrontal cortex, reticular cortex [RC], hippocampus [HC], hypothalamus [HT], medulla oblongata [OB], neuroblastoma [N2A], and murine melanoma [B16]; Figure S1E). Even within this subset, we found that TOBF1 expression was highest in mESCs, further corroborating its identity as a bona fide ESC marker. A recent report has suggested that TOBF1 is expressed in non-stem cells in mice and that it regulates gastric epithelial differentiation. This suggests that TOBF1 expression might be heterogeneous and that it has additional tissue-specific roles.³⁸

TOBF1-deficient mESCs exhibit destabilization of pluripotency

In our previous study, we identified that TOBF1 interacts with lncRNA Panct1 and forms bright nuclear puncta at the G1 cell-cycle phase. Although this localization pattern could be extrapolated to chromosomal territories both by electron microscopy and chromatin immunoprecipitation (ChIP), our results did not establish the functional role of TOBF1 as a distinct regulator of transcription.

Since TOBF1 has a prominent cell-cycle-specific localization pattern, we next inquired if this was influenced by gross changes in TOBF1 levels across the cell cycle. We sorted R1/E mESCs using the FUCCI (fluorescent, ubiquitination-based cell-cycle indicator) system for distinguishing the G1 and non-G1 phases of the cell cycle.^{54,55} We noticed a small (~1.5-fold) increase in TOBF1 mRNA levels in early G1 phase as compared with non-G1-phase cells (Figure 2A), suggesting that TOBF1 levels might undergo a low level of shuttling between its G1 versus non-G1 expression patterns.

We next turned our attention to the possible role of TOBF1 in regulating the ESC state through perturbation experiments. We adopted two CRISPR-based approaches to either knock down (CRISPR interference [CRISPRi])^{56,57} or KO (CRISPR-based dual-single guide RNA [sgRNA]-mediated deletion)⁵⁸ TOBF1 in R1/E WT mESCs. For TOBF1 knockdown, we used dFnCas9 fused with the Krüppel-associated box (KRAB) domain^{59–61} along with sgRNAs targeting the promoter of TOBF1 locus (Figure S2A). We observed that 48 h after transfection of CRISPRi constructs, a ~70% reduction in TOBF1 mRNA levels was seen. Importantly, a concomitant reduction in classical pluripotency and pluripotency-associated markers such as *Pou5f1*, *Sox2*, *Klf4*, *Nanog*, *Zfp42*, and *Zscan4* was observed, suggesting that these cells were exiting from their pluripotent state

(B) Schematic diagram of the dual-single guide RNA (sgRNA)-based CRISPR targeting of exons 2, 3, and 4 of *Tobf1* gene. Representative image of western blot showing TOBF1 protein expression in R1E WT mESCs and TOBF1 KO cells as ~84 kDa protein. β -Tubulin taken as loading control. Bar plot with error bars showing SD of the quantification of the western blot with three independent replicates. ***p < 0.0001 (Student's t test).

(C) qRT-PCR showing relative fold change (log2) of mRNA levels of different pluripotency markers (*Pou5f1*, *Sox2*, *Klf4*, *Nanog*, *Zfp42*, *Zscan4*) upon TOBF1 KO as compared with R1/E WT control cells. All values normalized with β -actin. Error bars indicate the SD of three independent replicates. *p < 0.05, **p < 0.001, ***p < 0.0001 (Student's t test).

(D) Representative light microscope grayscale images showing distinct morphological differences between R1/E WT cells and TOBF1 KO cells. Undifferentiated R1/E WT mESCs form round intact colonies, but TOBF1 KO cells show more spread-out flat morphology. Scale bar: 100 μ m.

(E) qRT-PCR showing relative fold change (log2) of mRNA levels of *Tobf1* and other pluripotency markers (*Pou5f1*, *Sox2*, *Klf4*, *Nanog*, *Zfp42*, *Zscan4*) in TOBF1 overexpression, TOBF1 KO, and TOBF1 rescue conditions as compared with R1/E WT cells. All values are normalized with β -actin. Error bars indicate the SD of two independent replicates.

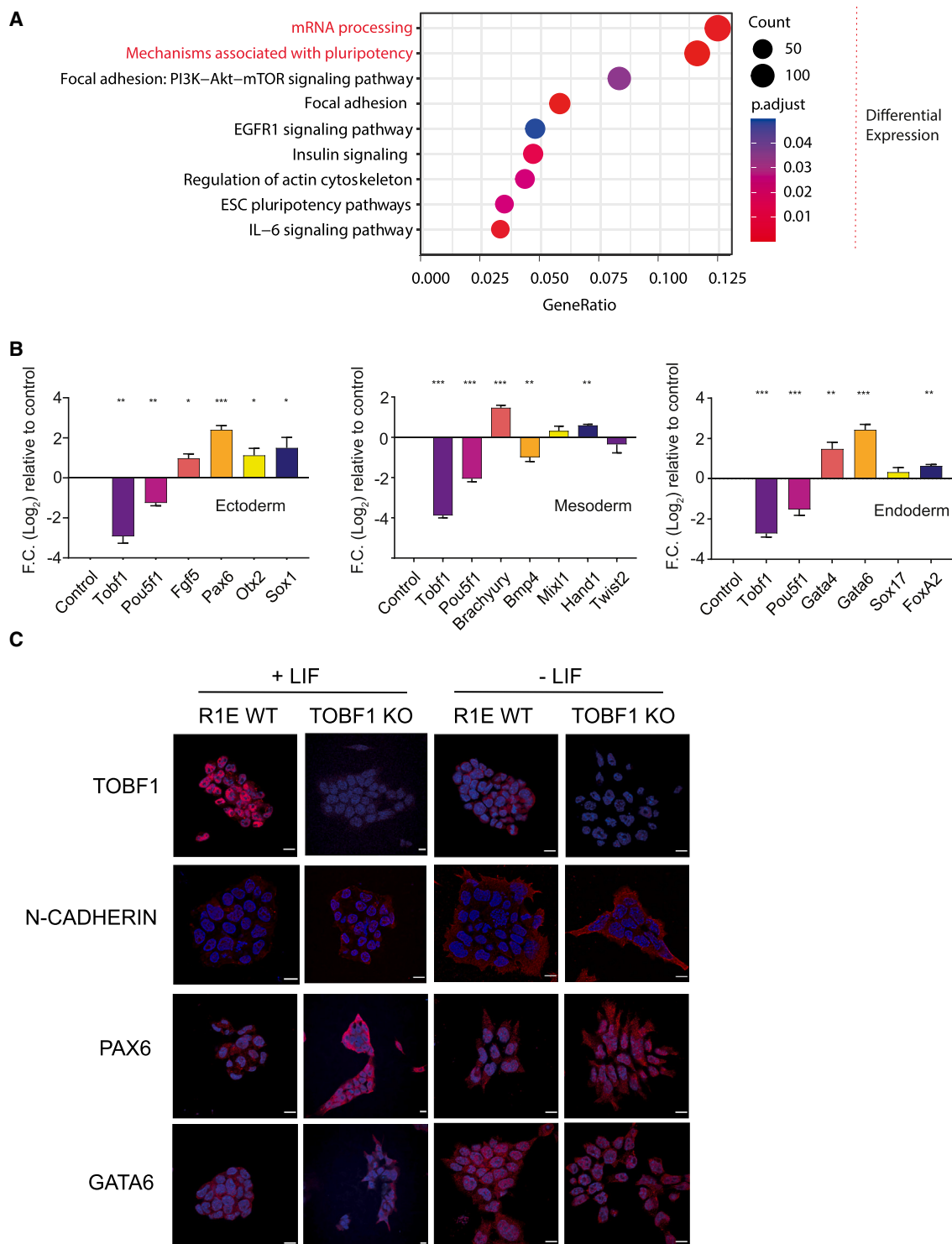


Figure 3. TOBF1 perturbation affects global transcript levels associated with pluripotency and lineage commitment

(A) Dot plot showing the enrichment of the top pathways of the differentially expressed genes from RNA-seq. Dark red represents a high significant p value, and dot is scaled with respect to number of genes involved in pathways.

(B) qRT-PCR showing the relative mRNA fold levels of primed ESCs/ectodermal (*Fgf5*, *Pax6*, *Sox1*, *Otx2*), mesodermal (*Brachyury*, *Bmp4*, *Mixl1*, *Hand1*, *Twist2*), and endodermal (*Gata4*, *Gata6*, *Sox17*, *FoxA2*) lineage markers in TOBF1 KO as compared with R1/E WT cells when these cells are cultured in defined trilineage

(legend continued on next page)

(Figure S2B). This observation was similar to esiRNA-mediated knockdown studies, where TOBF1 mRNA was targeted and similar reductions in *Pou5f1* and *Klf4* mRNA levels were seen. Both of these results confirm that TOBF1 perturbation impairs the expression of regulators of pluripotency in mESCs.

Having established the connection between TOBF1 mRNA levels and markers of mESC pluripotency, we next proceeded to investigate mESCs lacking TOBF1. To this end, we generated a CRISPR-mediated stable TOBF1 KO in R1/E mESCs using sgRNAs targeting exons 2, 3, and 4. We observed efficient KO of TOBF1 expression both at the mRNA and protein levels (Figure 2B). Similar to the knockdown experiments, upon TOBF1 KO, the expressions of key pluripotency regulators such as *Pou5f1*, *Sox2*, *Klf4*, *Nanog*, *Zfp42*, and *Zscan4* were all downregulated (Figure 2C). Visibly, TOBF1 KO mESCs displayed a flattened morphological phenotype comparable to differentiated cells (Figure 2D), whereas R1E WT mESCs showed distinct colonies. Taken together with our earlier observations, we conclusively show that TOBF1 perturbation through transcriptional repression of the gene promoter, genetic KO of the gene, or RNA interference all result in altering the pluripotent state of mESCs.

Because TOBF1 KO cells showed reduced expression of pluripotency-associated genes, next we investigated whether this phenotype could be rescued by exogenous overexpression of TOBF1. Upon overexpressing TOBF1 through a constitutive promoter, we observed that apart from *Nanog* and *Zscan4*, the expression of all other pluripotency genes (*Pou5f1*, *Sox2*, *Klf4*, and *Zfp42*) switched from a downregulated state to an upregulated state (Figure 2E). This further strengthened the association of TOBF1 with the core pluripotency network in mESCs, and TOBF1 overexpression shows a similar phenotype as rescue but with a higher fold change. We then sought to understand whether modulating TOBF1 brings any changes in the cell-cycle pattern of the ESCs, where exit from pluripotency results in reduction in the S-phase population.^{62–65} Interestingly, upon TOBF1 rescue, the proportion of S-phase cells increased (Figure S2C), suggesting that the exogenous expression of TOBF1 in KO cells could rescue its phenotype and in turn induce self-renewal capacity.

TOBF1 perturbation affects global transcript levels associated with pluripotency and lineage commitment

Having established the connection between TOBF1 and mESC pluripotency, we investigated how TOBF1 KO influenced the genome-wide transcriptomic profile through total RNA sequencing (RNA-seq). Importantly, because the nuclear puncta phenotype and the association with splicing regulators were prominently observed in G1 cell-cycle-sorted TOBF1 KO cells, we focused on this phase for studying transcriptomic changes.

We used the FUCCI system to sort G1-specific mESC population in TOBF1 KO cells and observed that 4,644 genes (2,253

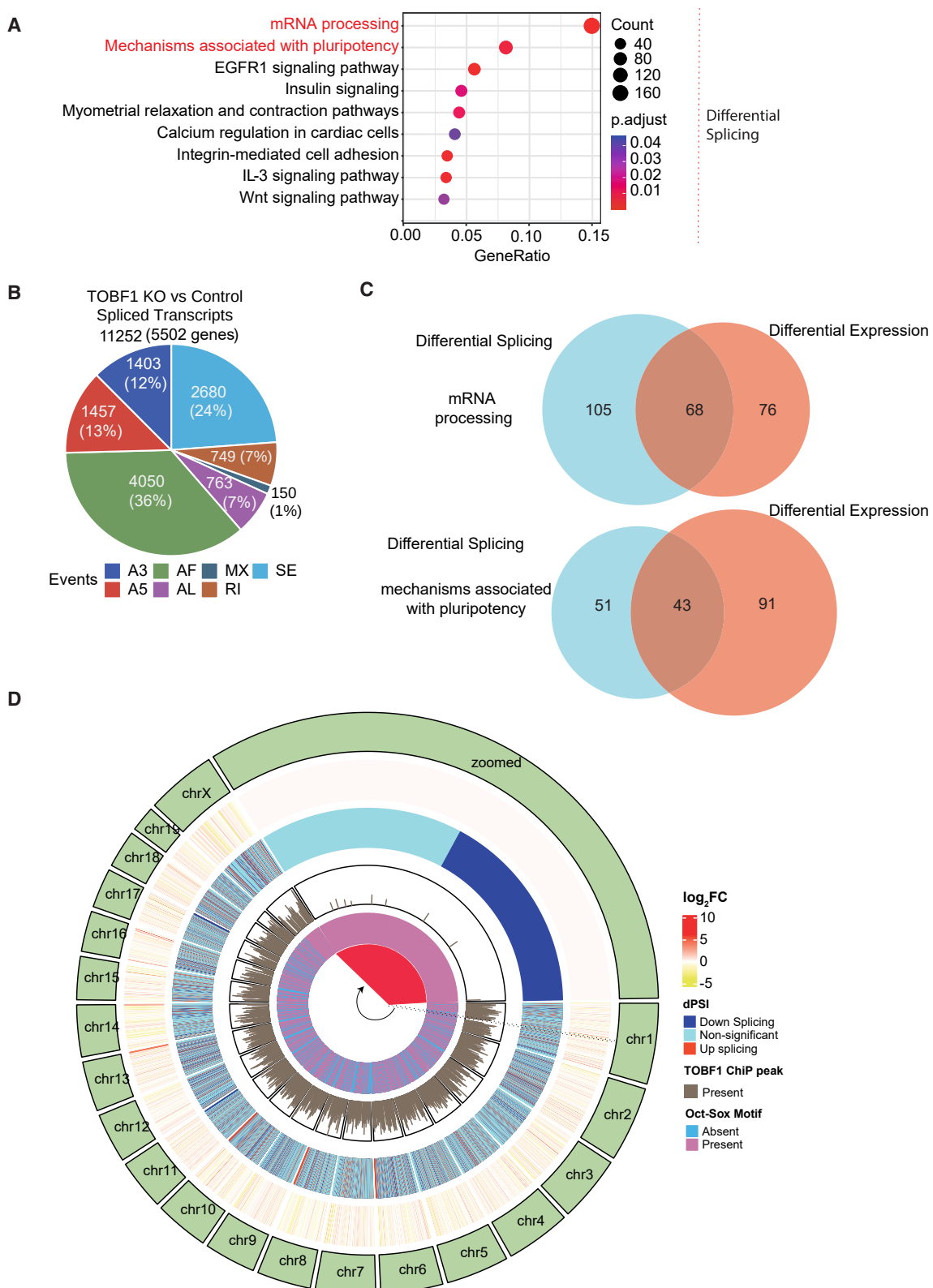
upregulated and 2,391 downregulated) were differentially expressed between TOBF1 KO and WT with false discovery rate (FDR) <0.05 (Table S2). We performed pathway analysis of these genes and found that the top two pathways enriched ($p < 0.01$) were “mRNA processing” and “mechanisms associated with pluripotency” (Figure 3A; Table S3). Although it was expected that pluripotency genes would be differentially expressed upon TOBF1 KO based on our qRT-PCR results, mRNA processing genes being affected signified a hitherto unexplained role of the protein that we subsequently investigated. Interestingly, among the topmost genes that showed the most significant fold reduction were *Klf4*, *Lefty2*, *Lefty1*, *c-Myc*, *Spry4*, *Sox2*, *Klf5*, *Klf12*, and *Bmp4*, all having known roles in regulating mESC identity.^{66–77} In contrast, lineage commitment factors such as *Dll1* and transforming growth factor β (TGF- β) signaling factor *Smad6*^{78,79} were significantly upregulated (Figure S2D). We selected a subset of the top differentially expressed transcripts from the TOBF1 RNA-seq results (*Klf4*, *c-Myc*, *Lefty1*, *Lefty2*, *Spry4*, *Klf5*, *Klf12*, *Bmp4*, *Trh*, *Egr1*, *Dll1*, *Smc1b*, *Incenc1*, *A2m*, *Smad6*) and successfully validated several of them using qRT-PCR (Figure S2E). In addition, we found *Nodal*, another bona fide pluripotency marker⁸⁰ downregulated upon TOBF1 KO (Figure S2E). Through these results, we concluded that TOBF1 KO leads to global transcriptome-wide changes that cumulatively result in an alteration from pluripotent state.

Next, we investigated whether differentiated TOBF1 KO cells have an increased expression of lineage commitment factors. To this end, we differentiated TOBF1 KO ESCs in trilineage differentiation media and observed that markers corresponding to all three germ layers (*Fgf5* for primed ESCs; *Pax6*, *Otx2*, and *Sox1* for ectoderm; *Brachury*, *Mixl1*, *Hand1*, and *Twist2* for mesoderm; and *Gata4*, *Gata6*, *Sox17*, and *FoxA2* for endoderm)^{81–90} showed enhanced expression (Figure 3B). These results suggested that TOBF1 KO primes ESCs to enter into a differentiated state.

As a corollary, we also tested whether subjecting TOBF1 KO cells to spontaneous differentiation by removal of leukemia inhibitory factor (LIF) enhanced the expression of lineage commitment markers in these cells. Using qRT-PCR, we confirmed that lineage markers corresponding to all three germ layers (*Brachury*, *Hand1*, *Twist2*, and *Mixl1* for mesoderm; *Otx2*, *Sox1*, and *Pax6* for ectoderm; and *Gata4*, *Gata6*, *Sox17*, and *FoxA2* for endoderm) were overexpressed over control (Figure S3A). This was further confirmed at the protein expression level using IF for PAX6 (ectoderm), n-CADHERIN (mesoderm), and GATA6 (endoderm) (Figures 3C and S3B). Interestingly, we observed that upon spontaneous differentiation, TOBF1 KO leads to a comparatively higher expression of mesodermal markers, suggesting that genes involved in the mesodermal lineage might be strongly affected upon TOBF1 KO. In concordance with this, among the RNA-seq hits, *Lefty1* and *Lefty2*, both of which are prominent members of the TGF- β pathway and

differentiation media. *Pou5f1* is taken as a negative marker for differentiation. All values normalized with β -actin. Error bars indicate the SD of three independent replicates. * $p < 0.05$, ** $p < 0.001$, *** $p < 0.0001$ (Student's t test).

(C) Representative images of IF showing expression of TOBF1, n-CADHERIN, PAX6, and GATA6 (shown in red) in R1/E WT mESCs and TOBF1 KO cells cultured in regular media (+LIF, 20% FBS) and spontaneous differentiation media (−LIF, 10% FBS). DNA is counterstained with DAPI. Whiskers indicate positive and negative deviations from mean ($n = 40$ cells). Scale bar: 10 μ m.



(legend on next page)

regulate mesoderm formation in vertebrates,^{91,92} emerged as highly differentially expressed upon TOBF1 KO (Figures S2D and S2E).

Absence of TOBF1 alters mRNA splicing patterns in mESCs

Pathway analysis of the differentially expressed genes upon TOBF1 KO revealed that genes responsible for mRNA processing were even more significantly altered than pluripotency genes. Although mRNA processing involves a multitude of pathways, including capping, methylation, splicing, 3' end processing, etc., we decided to focus on the role of TOBF1 in AS because interactome studies had already established its link with splicing factors (Figure 1A).

TOBF1 KO cells showed 11,252 events (from 5,502 genes) (difference in percent splicing inclusion, (dPSI) > |0.10|) that had undergone differential AS. Strikingly, the top two cellular pathways that these events contributed to (based on the number of enriched genes) were “mRNA processing” and “mechanisms associated with pluripotency,” both of which were enriched among differentially expressed transcripts as well (Figures 4A and 4B; Tables S4 and S5). Apart from these two pathways, EGFR1 signaling and insulin signaling also featured in the top pathways enriched among differentially spliced transcripts.

The enrichment of common pathways related to mRNA processing and ESC pluripotency suggested that there was a potential overlap of transcripts between the two pathways. Indeed, 27% of transcripts (68 out of 249) involved in mRNA processing and 23% of transcripts (43 out of 185) involved in ESC pluripotency (Figure 4C) were both significantly differentially expressed and differentially spliced.

TOBF1 forms discrete cotranscriptional splicing (CTS) hubs at sites of OCT-SOX motifs

Considering that TOBF1 is a global regulator of splicing and transcription, we considered its punctate localization in mESC nuclei during the early G1 phase as a possible hub for CTS. This process, which happens in close spatially and temporally associated territories, has been reported in multiple systems, although its role in ESCs has not been reported to our knowledge.

Our earlier studies on the association of *Panct1* and TOBF1 at OCT-SOX motifs had suggested the possible binding of TOBF1 to chromatin in the bright nuclear puncta in early G1 cells.³⁷ In this study, we identified TOBF1 as a component of the spliceosome complex whose perturbation led to global splicing changes. Importantly, this also led to transcriptional changes, which finally culminated in loss of pluripotency. The three obser-

vations, namely DNA occupancy, splicing modulation, and transcriptional regulation, are all hallmarks of CTS and indicate the formation of local factories or hubs of such coordinated events that are potentially scaffolded through lncRNAs like *Panct1*. Incidentally, the highly abundant lncRNA *Malat1* is known to regulate AS events through localization to NSs and interaction with splicing factors through conserved motifs in its secondary structure^{93,94}.

To investigate whether the two TOBF1 events (DNA binding and CTS) are indeed associated, we overlaid the three datasets of chromatin occupancy, splicing events, and differentially expressed transcripts upon KO across the whole-mouse genome and represented in the form of circos plot (Figure 4D; Table S6). We observed that TOBF1 chromatin occupancy was strongly correlated with sites of CTS. Moreover, both of these events also strongly correlated with the presence of the OCT-SOX motifs on DNA. Taken together, this suggested that TOBF1 recruitment to DNA potentially mediated through lncRNAs like *Panct1* leads to rapid assembly of local nuclear regions (represented by puncta) where CTS events happen.

TOBF1 KO leads to alternative isoform usage and loss of SRSF1

The presence of common transcripts that were both alternatively spliced and differentially expressed appeared surprising considering that transcription regulation and AS of the same gene proceed through different mechanisms.^{95–97} Further, the consequence of TOBF1 perturbation upon pluripotency appeared to be a cumulative effect of multiple altered ESC-related pathways that all contributed to the exit from undifferentiated state. For example, the highly significant AS events included KLF4, an important pluripotency regulator; JARID2, a polycomb-repressive complex 2 (PRC2) component that regulates ESC-specific transcriptional signatures^{98,99}; and CTCF, a multifunctional protein that mediates long-range interactions modulating pluripotency.^{100,101} In addition to these, several other factors that are known to be important regulators of ESC pluripotency such as ESRRB, HDAC1 and -4, DNMT3A, etc., which function through multiple distinct pathways,^{102–107} were also alternatively spliced (Table S5). Thus, from the KO data alone, we were not able to pinpoint the primary factor that orchestrated the downstream splicing and transcriptional regulation cascade that eventually led to the ESC phenotype.

To uncover the primary target of TOBF1-mediated splicing that affected global ESC splicing changes and loss of pluripotency, we hypothesized that such a transcript would undergo different splicing patterns in TOBF1 overexpression versus KO conditions. To this end, we overexpressed TOBF1 in mESCs

Figure 4. Loss of TOBF1 alters mRNA splicing patterns in mESCs

- (A) Dot plot of WikiPathways showing the enrichment of the top pathways of the differentially alternatively spliced events from RNA-seq. Dark red represents a high significant p value and dot scaled with respect to the number of genes involved in pathways.
- (B) Pie chart showing distribution of differential alternatively spliced events such as alternative 3' splice site (A3), alternative first exon (AF), mutually exclusive (MX), skipped exon (SE), alternative 5' splice site (A5), and retained intron (RI) (11,252 transcripts out of 5,502 genes) in TOBF1 KO and R1/E WT control cells.
- (C) Venn diagram showing overlapping transcripts count between differentially spliced transcripts and differentially expressed transcripts in mRNA processing pathways and mechanisms associated with pluripotency pathways enriched in the Gene Ontology enrichment pathway analysis.
- (D) Circos plot showing TOBF1 chromatin occupancy is strongly correlated with sites of CTS, and these events are also strongly correlated with the presence of the OCT-SOX motifs on DNA.

and performed RNA-seq to analyze differentially spliced genes in the G1 phase of the cell cycle (using the FUCCI reporter system described earlier).

TOBF1 overexpression uncovered 13,116 events (from 6,107 genes) ($dPSI > |0.10|$) that had undergone differential AS (Table S7). Among these genes, we looked for commonly spliced transcripts between the TOBF1 KO and overexpression conditions (relative to control). Our analysis uncovered 17 events (13 genes) that showed AS behavior between the two datasets, suggesting a direct TOBF1-mediated control of their splicing (Figure 5A; Table S8). Strikingly, among the genes that showed such a response, SRSF1, a predominant splicing factor responsible for AS of mRNAs in different cell types, stood out. SRSF1 has been studied in multiple contexts ranging from post-transcriptional splicing regulation in cancer and RNA associated with cell-cycle regulation and chromosomal segregation.^{108–110} Studies have also shown that SRSF1 is required for proper postnatal development in mice and that SRSF1 also regulates human ESC fate by regulating histone modifications.^{111–113} Since SRSF1 was the only gene that was previously shown to regulate ESC identity, we studied it further.

Closer inspection of the SRSF1 splicing pattern upon TOBF1 perturbation revealed an interesting pattern of expression of the constituent isoforms. *Srsf1* isoforms 202, 205, and 201 code for the functional protein, while 204 and 207 undergo nonsense-mediated decay. Isoforms 206 and 203 do not code for a functional protein (Ensembl genome browser). TOBF1 KO leads to a downregulation of the predominant protein coding isoform 202 and upregulates isoforms 204 and 203 (Figure 5B). TOBF1 overexpression, on the other hand, did not cause such striking changes in the isoform usage.

As the SRSF1 isoform expression patterns indicated that the protein was possibly downregulated upon TOBF1 KO, we validated the AS of the transcript using qRT-PCR (of a common region in exon 4 shared between isoform 202 and 205) and observed that the *Srsf1* protein-coding isoform was strongly downregulated (up to ~91%) in TOBF1 KO cells (Figure 5C). Finally, we performed a western blot and established that SRSF1 protein is lost upon TOBF1 KO (Figure 5D).

Interestingly, in a recent report, SRSF1 has also been implicated in the usage of negative autoregulation through AS to maintain its levels inside cells and concomitantly affect multiple splicing patterns and eventual cellular fate.¹¹⁴ Our results suggest that TOBF1 in mESCs is involved in the regulation of SRSF1 expression through regulation of its isoform usage. This in turn sets in motion global changes in splicing and transcription that ultimately lead to destabilization of self-renewal properties of these cells.

DISCUSSION

We propose a model whereby TOBF1 interacts with other mRNA processing and splicing factors to promote the AS of different transcripts essential for the regulation of ESCs. Predominant among its targets is the canonical splicing factor SRSF1, whose alternative isoform usage leads to downregulation of the protein and concomitant changes in the splicing of ESC-specific transcripts and their expression. Eventually, this leads to destabiliza-

tion of the pluripotent state. We also show that the recruitment of TOBF1 to chromatin at OCT-SOX motifs in early G1 phase suggests that TOBF1 may be a control switch for appropriate assembly of splicing factors and concomitant transcriptional regulation. Absence of TOBF1 resulted in the dissolution of such assemblies, thereby affecting multiple downstream pathways. In our splicing and expression data, we identified a myriad of ESC-specific genes, several of which function through independent pathways. Thus, TOBF1's role is upstream of canonical ESC-specific events, although they cumulatively affect pluripotency.

It is interesting to speculate what the role of TOBF1 might be in other cell types. For example, in mouse gastric epithelial cells, TOBF1 has been shown to suppress Wnt-related and Reg family genes, ultimately leading to epithelial renewal. Indeed, in our TOBF1 RNA-seq data, we did observe several genes involved in the Wnt pathway¹¹⁵ to be differentially expressed (such as downregulated *c-Myc* and *Fosl1* and upregulated *Wnt7b* and *Fzd2*, among others). However, our systematic study of chromatin association, cellular localization, and CTS reveals a more detailed functionality of TOBF1 that expands beyond the scope of specific pathways and suggests a more elaborate central role of TOBF1 in regulating stem cell fate, at least in mESCs. Nevertheless, it will be important to investigate if TOBF1's role in CTS is redundant in other cells, tissues, and organs. A starting point to investigate this might be human ESCs, where TOBF1 shows significant conservation.

In recent times, several groups have reported a strong association between lncRNAs and AS events, with particular emphasis on their disease relevance. In several instances, lncRNAs directly interact with splicing factors and cooperate with or hijack AS events. Some examples include TPM1-AS lncRNA with RBM4 and DGCR5 lncRNA with SRSF1, both of which have roles in progression of human esophageal cancer cells.^{116–118} Our studies highlight a similar cooperativity between the lncRNA *Panct1* and TOBF1 in the eventual formation of CTS hubs in mESCs. However, *Panct1* is poorly conserved across different species, although TOBF1 shares significant homology between mouse, human, and other mammals. This suggests that additional lncRNAs might phenocopy *Panct1* in assembling such CTS factories. Also, as seen for other lncRNAs, local structural motifs such as g-quadruplexes or -triplexes in RNAs might be the functional motifs linking such transcripts with CTS events.^{119–121} Systematic dissection of such motifs in *Panct1* and other TOBF1-interacting lncRNAs will shed light on how such cooperativity might occur.

A consistently intriguing observation in our study has been the bright G1 puncta where all these events occur. As these puncta bring together multiple proteins, DNA, and RNA in close proximity, they suggest a dynamic assembly reminiscent of biomolecular liquid condensates. Our previous study showed TOBF1 puncta to exhibit dynamic coalescing properties akin to liquid-liquid phase separation. In a recent paper, the NS marker SRRM2 has been shown to exhibit similar properties in HEK293T cells all across the cell cycle.^{49,122} Because SRRM2 interacts physically with TOBF1, the TOBF1 puncta and associated CTS hubs in early G1 phase in mESCs possibly reflect phase-separated condensates. Further studies through

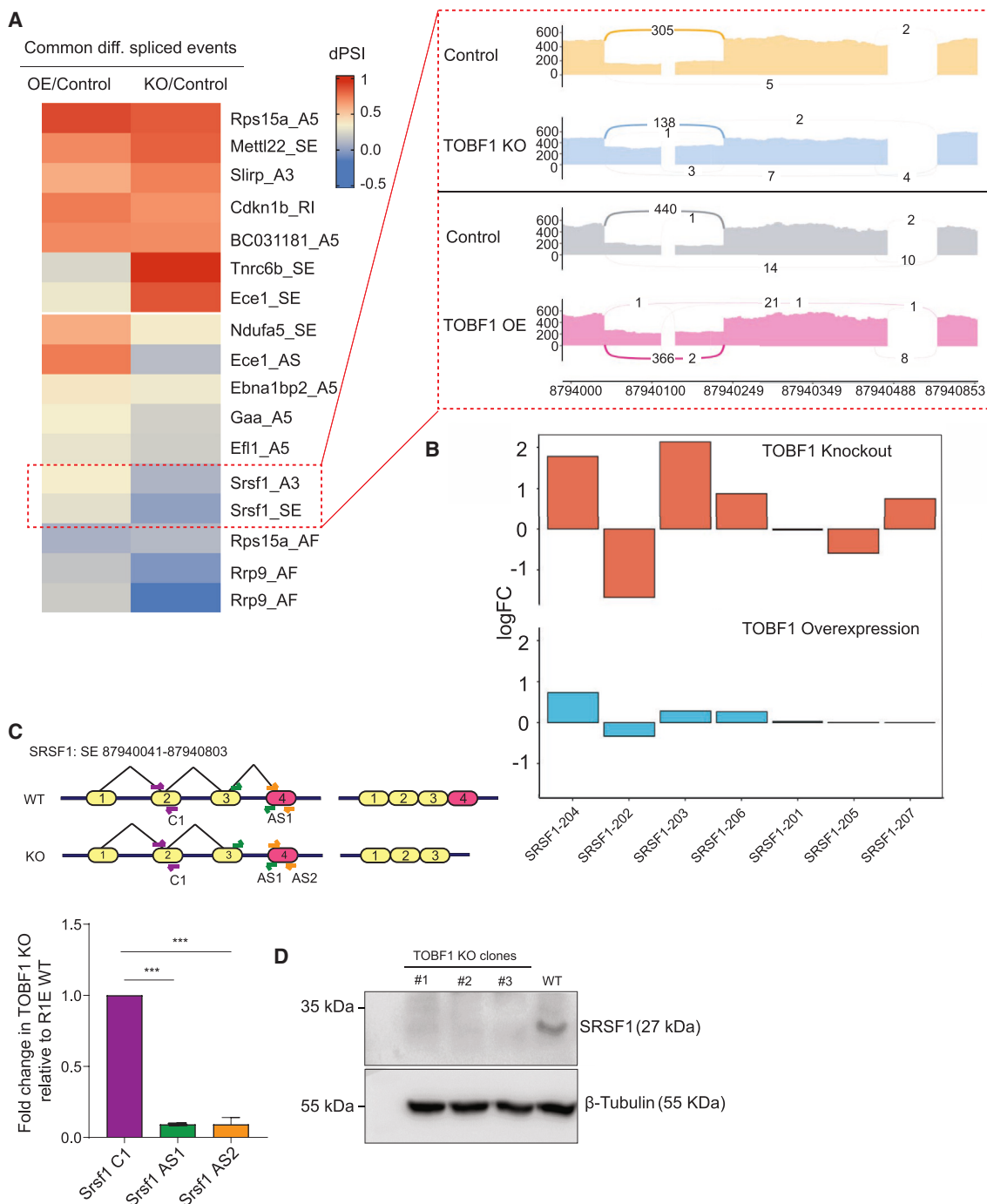


Figure 5. TOBF1-mediated AS of *Srsf1* in mESCs leads to global changes in mRNA splicing and expression

(A) Heatmap showing the common differential alternatively spliced transcripts in TOBF1 overexpression and KO conditions when compared with R1/E WT cells. Inset showing the sashimi plot of the genomic coordinates ch11:87,940,041–87,940,803 that represents the differential exon-skipping pattern of *Srsf1* transcript.

(B) Bar plot showing the differential *Srsf1* isoforms expression in TOBF1 overexpression and KO conditions.

(C) Schematic diagram showing the differences in the splicing pattern in exon 4 of *Srsf1* gene transcript isoforms in TOBF1 KO and R1E WT mESCs. qRT-PCR showing the relative mRNA fold changes using two different primer sets (AS1, AS2) to validate the splicing of exon 4 of *Srsf1* by taking the constitutive exon as the control (C1) primer set. All values are normalized with β -actin. Error bars indicate the SD of three independent replicates. * $p < 0.05$, ** $p < 0.01$, *** $p < 0.0001$ (Student's t test).

(D) Representative image of western blot showing the expression of SRSF1 in TOBF1 KO cells in three biological replicates as compared with R1E WT cells.

abrogation of defined TOBF1 motifs would be necessary to conclusively establish the identity of such condensates and the role of local protein-RNA contacts in maintaining them.

Although *Panct1* is very poorly conserved among vertebrates, TOBF1 shares a very high homology with multiple species, underscoring its role in splicing and transcriptional regulation, among others. Considering that it is largely uncharacterized to date, future studies might reveal non-canonical roles that go over and beyond what we identified in this work.

Limitations of the study

In this study, we have grown mESCs in FBS+LIF, which often does not represent the ground state of pluripotency. Although we performed a set of experiments to show that the pluripotency markers show similar downregulation in the ground/naive state when grown in 2i media, a more in-depth study focusing on the two states might dissect the role of TOBF1 with far greater granularity in these cells (Figure S4A). Another limitation of this study is the absence of a greater mechanistic understanding of SRSF1 on pluripotency. As there are limited data in published literature, we focused on one candidate, *Pbx1*, whose two isoforms, *Pbx1a* and *Pbx1b*, are alternatively spliced during differentiation.^{123,124,125,113,126} We did observe that the *Pbx1b* isoform shows a slightly increased expression as compared with *Pbx1a* in TOBF1 KO cells and that the overall expression of *Pbx1* is significantly reduced in TOBF1 KO as compared with R1E WT. However, the details of the mechanism through which these proteins act has been left unexplored in this study (Figures S4B and S4C).

STAR★METHODS

Detailed methods are provided in the online version of this paper and include the following:

- KEY RESOURCES TABLE
- RESOURCE AVAILABILITY
 - Lead contact
 - Materials availability
 - Data and code availability
- EXPERIMENTAL MODEL AND STUDY PARTICIPANT DETAILS
 - Cell lines and cell culture
- METHOD DETAILS
 - Cells transfection and harvesting
 - Cells synchronization
 - Affinity pull-down and mass spectrometry
 - Generating TOBF1 KO cells
 - Over-expression of TOBF1
 - RNA extraction methods
 - RNA sequencing analysis
 - qRT-PCR
 - Western blot
 - Immunofluorescence (IF)
 - Immunoprecipitation (IP)
 - Cell cycle assay
- QUANTIFICATION AND STATISTICAL ANALYSIS

SUPPLEMENTAL INFORMATION

Supplemental information can be found online at <https://doi.org/10.1016/j.celrep.2023.113177>.

ACKNOWLEDGMENTS

The authors thank Dr. Amrita Singh and Ms. Rhythm Phutela from CSIR-IGIB for designing and creating the dual-sgRNA SpCas9 plasmid and the dFnCas9-KRAB plasmid, respectively, which were used for TOBF1 KO and CRISPRi experiments. The authors are grateful to all members of the Chakraborty and Maiti labs for helpful discussions and suggestions and to Dr. Shakti Sagar and Ms. Vandana Singh from CSIR IGIB for help with the microscopy experiments. This study was funded by an EMBO Young Investigator Award (GAP0252) and a Department of Biotechnology grant (GAP0188) to D.C. The mass spectrometry (MS) experiments were funded by EU FP7 grant SyBoSS (242129) to F.B. and C.C. The Novo Nordisk Foundation Center for Protein Research is financially supported by the Novo Nordisk Foundation (NNF14CC0001).

AUTHOR CONTRIBUTIONS

M.A., S.M., and D.C. conceived, designed, and interpreted the experiments. A.H.A. analyzed and provided bioinformatics support for data interpretation. L.D. and F.B. analyzed and interpreted data from BAC-tagged cell lines. V.I. and C.C. performed and analyzed data from affinity purification studies. D.P. performed experiments with FUCCI-tagged ESC lines. M.A. and D.C. wrote the manuscript with input from all other authors.

DECLARATION OF INTERESTS

The authors declare no competing interests.

Received: February 8, 2023

Revised: June 28, 2023

Accepted: September 11, 2023

Published: September 25, 2023

REFERENCES

1. Evans, M.J., and Kaufman, M.H. (1981). Establishment in culture of pluripotential cells from mouse embryos. *Nature* 292, 154–156.
2. Martin, G.R. (1981). Isolation of a pluripotent cell line from early mouse embryos cultured in medium conditioned by teratocarcinoma stem cells. *Proc. Natl. Acad. Sci. USA* 78, 7634–7638.
3. Bradley, A., Evans, M., Kaufman, M.H., and Robertson, E. (1984). Formation of germ-line chimaeras from embryo-derived teratocarcinoma cell lines. *Nature* 309, 255–256.
4. Wobus, A.M., and Boheler, K.R. (2005). Embryonic stem cells: prospects for developmental biology and cell therapy. *Physiol. Rev.* 85, 635–678.
5. Boyer, L.A., Lee, T.I., Cole, M.F., Johnstone, S.E., Levine, S.S., Zucker, J.P., Guenther, M.G., Kumar, R.M., Murray, H.L., Jenner, R.G., et al. (2005). Core transcriptional regulatory circuitry in human embryonic stem cells. *Cell* 122, 947–956.
6. Loh, Y.-H., Wu, Q., Chew, J.-L., Vega, V.B., Zhang, W., Chen, X., Bourque, G., George, J., Leong, B., Liu, J., et al. (2006). The Oct4 and Nanog transcription network regulates pluripotency in mouse embryonic stem cells. *Nat. Genet.* 38, 431–440.
7. Takahashi, K., and Yamanaka, S. (2006). Induction of pluripotent stem cells from mouse embryonic and adult fibroblast cultures by defined factors. *Cell* 126, 663–676.
8. Meshorer, E., Yellajosula, D., George, E., Scambler, P.J., Brown, D.T., and Misteli, T. (2006). Hyperdynamic plasticity of chromatin proteins in pluripotent embryonic stem cells. *Dev. Cell* 10, 105–116.

9. Efroni, S., Duttagupta, R., Cheng, J., Dehghani, H., Hoeppner, D.J., Dash, C., Bazett-Jones, D.P., Le Grice, S., McKay, R.D.G., Buetow, K.H., et al. (2008). Global transcription in pluripotent embryonic stem cells. *Cell Stem Cell* 2, 437–447.
10. Mao, J., Zhang, Q., Deng, W., Wang, H., Liu, K., Fu, H., Zhao, Q., Wang, X., and Liu, L. (2017). Epigenetic Modifiers Facilitate Induction and Pluripotency of Porcine iPSCs. *Stem Cell Rep.* 8, 11–20.
11. Bulut-Karslioglu, A., Macrae, T.A., Oses-Prieto, J.A., Covarrubias, S., Perchard, M., Ku, G., Diaz, A., McManus, M.T., Burlingame, A.L., and Ramalho-Santos, M. (2018). The Transcriptionally Permissive Chromatin State of Embryonic Stem Cells Is Acutely Tuned to Translational Output. *Cell Stem Cell* 22, 369–383.e8.
12. Li, D., and Wang, J. (2020). Ribosome heterogeneity in stem cells and development. *J. Cell Biol.* 219, e202001108. <https://doi.org/10.1083/jcb.202001108>.
13. Young, R.A. (2011). Control of the embryonic stem cell state. *Cell* 144, 940–954.
14. Tsialikas, J., and Romer-Seibert, J. (2015). LIN28: roles and regulation in development and beyond. *Development* 142, 2397–2404.
15. Chen, Q., and Hu, G. (2017). Post-transcriptional regulation of the pluripotent state. *Curr. Opin. Genet. Dev.* 46, 15–23.
16. Ye, J., and Blelloch, R. (2014). Regulation of pluripotency by RNA binding proteins. *Cell Stem Cell* 15, 271–280.
17. Guallar, D., and Wang, J. (2014). RNA-binding proteins in pluripotency, differentiation, and reprogramming. *Front. Biol.* 9, 389–409.
18. Nilsen, T.W., and Graveley, B.R. (2010). Expansion of the eukaryotic proteome by alternative splicing. *Nature* 463, 457–463.
19. Licatalosi, D.D., and Darnell, R.B. (2010). RNA processing and its regulation: global insights into biological networks. *Nat. Rev. Genet.* 11, 75–87.
20. Salomonis, N., Schlieve, C.R., Pereira, L., Wahlquist, C., Colas, A., Zambon, A.C., Vranizan, K., Spindler, M.J., Pico, A.R., Cline, M.S., et al. (2010). Alternative splicing regulates mouse embryonic stem cell pluripotency and differentiation. *Proc. Natl. Acad. Sci. USA* 107, 10514–10519. <https://doi.org/10.1073/pnas.0912260107>.
21. Han, H., Braunschweig, U., Gonatopoulos-Pournatzis, T., Weatheritt, R.J., Hirsch, C.L., Ha, K.C.H., Radovani, E., Nabeel-Shah, S., Sterne-Weiler, T., Wang, J., et al. (2017). Multilayered Control of Alternative Splicing Regulatory Networks by Transcription Factors. *Mol. Cell* 65, 539–553.e7.
22. Lu, X., Göke, J., Sachs, F., Jacques, P.É., Liang, H., Feng, B., Bourque, G., Bubulya, P.A., and Ng, H.-H. (2013). SON connects the splicing-regulatory network with pluripotency in human embryonic stem cells. *Nat. Cell Biol.* 15, 1141–1152.
23. Lu, Y., Loh, Y.-H., Li, H., Cesana, M., Ficarro, S.B., Parikh, J.R., Salomonis, N., Toh, C.-X.D., Andreadis, S.T., Luckey, C.J., et al. (2014). Alternative splicing of MBD2 supports self-renewal in human pluripotent stem cells. *Cell Stem Cell* 15, 92–101.
24. Cieply, B., Park, J.W., Nakauka-Ddamba, A., Bebee, T.W., Guo, Y., Shang, X., Lengner, C.J., Xing, Y., and Carstens, R.P. (2016). Multiphasic and Dynamic Changes in Alternative Splicing during Induction of Pluripotency Are Coordinated by Numerous RNA-Binding Proteins. *Cell Rep.* 15, 247–255.
25. Venables, J.P., Lapasset, L., Gadea, G., Fort, P., Klinck, R., Irimia, M., Vignal, E., Thibault, P., Prinos, P., Chabot, B., et al. (2013). MBNL1 and RBFOX2 cooperate to establish a splicing programme involved in pluripotent stem cell differentiation. *Nat. Commun.* 4, 2480.
26. Wang, X., Ping, C., Tan, P., Sun, C., Liu, G., Liu, T., Yang, S., Si, Y., Zhao, L., Hu, Y., et al. (2021). hnRNPL controls pluripotency exit of embryonic stem cells by modulating alternative splicing of Tbx3 and Bptf. *EMBO J.* 40, e104729.
27. Xu, Y., Li, R., Zhang, K., Wu, W., Wang, S., Zhang, P., and Xu, H. (2018). The multifunctional RNA-binding protein hnRNP K is critical for the proliferation and differentiation of myoblasts. *BMB Rep.* 51, 350–355.
28. Qi, Z., Wang, F., Yu, G., Wang, D., Yao, Y., You, M., Liu, J., Liu, J., Sun, Z., Ji, C., et al. (2021). SRSF1 serves as a critical posttranscriptional regulator at the late stage of thymocyte development. *Sci. Adv.* 7, eabf0753. <https://doi.org/10.1126/sciadv.abf0753>.
29. Comiskey, D.F., Jr., Jacob, A.G., Singh, R.K., Tapia-Santos, A.S., and Chandler, D.S. (2015). Splicing factor SRSF1 negatively regulates alternative splicing of MDM2 under damage. *Nucleic Acids Res.* 43, 4202–4218.
30. Gao, Y., Vasic, R., and Halene, S. (2018). Role of alternative splicing in hematopoietic stem cells during development. *Stem Cell Investig.* 5, 26.
31. Vidigal, J.A., and Ventura, A. (2012). Embryonic stem cell miRNAs and their roles in development and disease. *Semin. Cancer Biol.* 22, 428–436.
32. Aich, M., and Chakraborty, D. (2020). Role of lncRNAs in stem cell maintenance and differentiation. *Curr. Top. Dev. Biol.* 138, 73–112.
33. Flynn, R.A., and Chang, H.Y. (2014). Long noncoding RNAs in cell-fate programming and reprogramming. *Cell Stem Cell* 14, 752–761.
34. Li, J.-H., Liu, S., Zheng, L.-L., Wu, J., Sun, W.-J., Wang, Z.-L., Zhou, H., Qu, L.-H., and Yang, J.-H. (2014). Discovery of Protein-lncRNA Interactions by Integrating Large-Scale CLIP-Seq and RNA-Seq Datasets. *Front. Bioeng. Biotechnol.* 2, 88.
35. Engreitz, J.M., Haines, J.E., Perez, E.M., Munson, G., Chen, J., Kane, M., McDonel, P.E., Guttman, M., and Lander, E.S. (2016). Local regulation of gene expression by lncRNA promoters, transcription and splicing. *Nature* 539, 452–455.
36. Chakraborty, D., Kappei, D., Theis, M., Nitzsche, A., Ding, L., Paszkowski-Rogacz, M., Surendranath, V., Berger, N., Schulz, H., Saar, K., et al. (2012). Combined RNAi and localization for functionally dissecting long noncoding RNAs. *Nat. Methods* 9, 360–362.
37. Chakraborty, D., Paszkowski-Rogacz, M., Berger, N., Ding, L., Mircetic, J., Fu, J., Iesmantavicius, V., Choudhary, C., Anastassiadis, K., Stewart, A.F., and Buchholz, F. (2017). lncRNA Panc1 Maintains Mouse Embryonic Stem Cell Identity by Regulating TOBF1 Recruitment to Oct-Sox Sequences in Early G1. *Cell Rep.* 21, 3012–3021.
38. Murakami, K., Terakado, Y., Saito, K., Jomen, Y., Takeda, H., Oshima, M., and Barker, N. (2021). A genome-scale CRISPR screen reveals factors regulating Wnt-dependent renewal of mouse gastric epithelial cells. *Proc. Natl. Acad. Sci. USA* 118, e2016806118. <https://doi.org/10.1073/pnas.2016806118>.
39. Lee, K.-M., Hsu, I.-W., and Tarn, W.-Y. (2010). TRAP150 activates pre-mRNA splicing and promotes nuclear mRNA degradation. *Nucleic Acids Res.* 38, 3340–3350.
40. Beli, P., Lukashchuk, N., Wagner, S.A., Weinert, B.T., Olsen, J.V., Baskcomb, L., Mann, M., Jackson, S.P., and Choudhary, C. (2012). Proteomic investigations reveal a role for RNA processing factor THRAP3 in the DNA damage response. *Mol. Cell* 46, 212–225.
41. Vohchodova, J., Barros, E.M., Savage, A.L., Liberante, F.G., Manti, L., Bankhead, P., Cosgrove, N., Madden, A.F., Harkin, D.P., and Savage, K.I. (2017). The RNA processing factors THRAP3 and BCLAF1 promote the DNA damage response through selective mRNA splicing and nuclear export. *Nucleic Acids Res.* 45, 12816–12833.
42. Miller, E.E., Kobayashi, G.S., Musso, C.M., Allen, M., Ishiy, F.A.A., de Caires, L.C., Jr., Goulart, E., Griesi-Oliveira, K., Zechi-Ceide, R.M., Richieri-Costa, A., et al. (2017). EIF4A3 deficient human iPSCs and mouse models demonstrate neural crest defects that underlie Richieri-Costa-Pereira syndrome. *Hum. Mol. Genet.* 26, 2177–2191.
43. Richards, M., Tan, S.-P., Tan, J.-H., Chan, W.-K., and Bongso, A. (2004). The transcriptome profile of human embryonic stem cells as defined by SAGE. *Stem Cell* 22, 51–64.
44. Cornella, N., Tebaldi, T., Gasperini, L., Singh, J., Padgett, R.A., Rossi, A., and Macchi, P. (2017). The hnRNP RALY regulates transcription and cell proliferation by modulating the expression of specific factors including the proliferation marker E2F1. *J. Biol. Chem.* 292, 19674–19692.

45. Legrand, J.M.D., Chan, A.-L., La, H.M., Rossello, F.J., Änkö, M.L., Fuller-Pace, F.V., and Hobbs, R.M. (2019). DDX5 plays essential transcriptional and post-transcriptional roles in the maintenance and function of spermatogonia. *Nat. Commun.* **10**, 2278.
46. Ingolia, N.T., Lareau, L.F., and Weissman, J.S. (2011). Ribosome profiling of mouse embryonic stem cells reveals the complexity and dynamics of mammalian proteomes. *Cell* **147**, 789–802.
47. Gabut, M., Bourdelais, F., and Durand, S. (2020). Ribosome and Translational Control in Stem Cells9, Cells. <https://doi.org/10.3390/cells9020497>.
48. Bakhmet, E.I., Nazarov, I.B., Gazizova, A.R., Vorobyeva, N.E., Kuzmin, A.A., Gordeev, M.N., Sinenko, S.A., Aksenov, N.D., Artamonova, T.O., Khodorkovskii, M.A., et al. (2019). hnRNP-K Targets Open Chromatin in Mouse Embryonic Stem Cells in Concert with Multiple Regulators. *Stem Cell.* **37**, 1018–1029.
49. Illek, i.A., Malszyczki, M., Lübke, A.K., Schade, C., Meierhofer, D., and Aktaş, T. (2020). SON and SRRM2 are essential for nuclear speckle formation. *Elife* **9**, e60579. <https://doi.org/10.7554/elife.60579>.
50. Lin, S., Coutinho-Mansfield, G., Wang, D., Pandit, S., and Fu, X.-D. (2008). The splicing factor SC35 has an active role in transcriptional elongation. *Nat. Struct. Mol. Biol.* **15**, 819–826.
51. Fu, X.D., and Maniatis, T. (1990). Factor required for mammalian spliceosome assembly is localized to discrete regions in the nucleus. *Nature* **343**, 437–441.
52. Buszczak, M., Signer, R.A.J., and Morrison, S.J. (2014). Cellular differences in protein synthesis regulate tissue homeostasis. *Cell* **159**, 242–251.
53. van Hoof, D., Krijgsveld, J., and Mummery, C. (2012). Proteomic Analysis of Stem Cell Differentiation and Early Development. *Cold Spring Harbor Perspect. Biol.* **4**, a008177. <https://doi.org/10.1101/cshperspect.a008177>.
54. Sakae-Sawano, A., Kurokawa, H., Morimura, T., Hanyu, A., Hama, H., Osawa, H., Kashiwagi, S., Fukami, K., Miyata, T., Miyoshi, H., et al. (2008). Visualizing spatiotemporal dynamics of multicellular cell-cycle progression. *Cell* **132**, 487–498.
55. Sladitschek, H.L., and Neveu, P.A. (2015). MXS-Chaining: A Highly Efficient Cloning Platform for Imaging and Flow Cytometry Approaches in Mammalian Systems. *PLoS One* **10**, e0124958.
56. Gilbert, L.A., Horlbeck, M.A., Adamson, B., Villalta, J.E., Chen, Y., Whitehead, E.H., Guimaraes, C., Panning, B., Ploegh, H.L., Bassik, M.C., et al. (2014). Genome-Scale CRISPR-Mediated Control of Gene Repression and Activation. *Cell* **159**, 647–661.
57. Alerasool, N., Segal, D., Lee, H., and Taipale, M. (2020). An efficient KRAB domain for CRISPRi applications in human cells. *Nat. Methods* **17**, 1093–1096.
58. Maddalo, D., Manchado, E., Concepcion, C.P., Bonetti, C., Vidigal, J.A., Han, Y.-C., Ogródowski, P., Crippa, A., Rekhtman, N., de Stanchina, E., et al. (2014). In vivo engineering of oncogenic chromosomal rearrangements with the CRISPR/Cas9 system. *Nature* **516**, 423–427.
59. Kearns, N.A., Genga, R.M.J., Enuameh, M.S., Garber, M., Wolfe, S.A., and Maehr, R. (2014). Cas9 effector-mediated regulation of transcription and differentiation in human pluripotent stem cells. *Development* **141**, 219–223.
60. Williams, R.M., Senanayake, U., Artibani, M., Taylor, G., Wells, D., Ahmed, A.A., and Sauka-Spengler, T. (2018). Genome and Epigenome Engineering CRISPR Toolkit for Modulation of -regulatory Interactions and Gene Expression in the Chicken Embryo. *Development* **145**. <https://doi.org/10.1242/dev.160333>.
61. Parsi, K.M., Hennessy, E., Kearns, N., and Maehr, R. (2017). Using an Inducible CRISPR-dCas9-KRAB Effector System to Dissect Transcriptional Regulation in Human Embryonic Stem Cells. *Methods Mol. Biol.* **1507**, 221–233.
62. Jones, S.M., and Kazlauskas, A. (2001). Growth-factor-dependent mitogenesis requires two distinct phases of signalling. *Nat. Cell Biol.* **3**, 165–172.
63. Singh, A.M., and Dalton, S. (2009). The cell cycle and Myc intersect with mechanisms that regulate pluripotency and reprogramming. *Cell Stem Cell* **5**, 141–149.
64. Lee, J., Go, Y., Kang, I., Han, Y.-M., and Kim, J. (2010). Oct-4 controls cell-cycle progression of embryonic stem cells. *Biochem. J.* **426**, 171–181.
65. Li, P., Ding, N., Zhang, W., and Chen, L. (2018). COPS2 Antagonizes OCT4 to Accelerate the G2/M Transition of Mouse Embryonic Stem Cells. *Stem Cell Rep.* **11**, 317–324.
66. Zhang, P., Andrianakos, R., Yang, Y., Liu, C., and Lu, W. (2010). Kruppel-like factor 4 (Klf4) prevents embryonic stem (ES) cell differentiation by regulating Nanog gene expression. *J. Biol. Chem.* **285**, 9180–9189.
67. Kim, D.-K., Cha, Y., Ahn, H.-J., Kim, G., and Park, K.-S. (2014). Lefty1 and lefty2 control the balance between self-renewal and pluripotent differentiation of mouse embryonic stem cells. *Stem Cell Dev.* **23**, 457–466.
68. Meno, C., Gritsman, K., Ohishi, S., Ohfuri, Y., Heckscher, E., Mochida, K., Shimono, A., Kondoh, H., Talbot, W.S., Robertson, E.J., et al. (1999). Mouse Lefty2 and zebrafish antivin are feedback inhibitors of nodal signaling during vertebrate gastrulation. *Mol. Cell* **4**, 287–298.
69. Liu, X., Huang, J., Chen, T., Wang, Y., Xin, S., Li, J., Pei, G., and Kang, J. (2008). Yamanaka factors critically regulate the developmental signaling network in mouse embryonic stem cells. *Cell Res.* **18**, 1177–1189.
70. Varlakhanova, N.V., Cotterman, R.F., deVries, W.N., Morgan, J., Donahue, L.R., Murray, S., Knowles, B.B., and Knoepfler, P.S. (2010). myc maintains embryonic stem cell pluripotency and self-renewal. *Differentiation* **80**, 9–19.
71. Lee, J.-Y., Park, S., Kim, K.-S., Ko, J.-J., Lee, S., Kim, K.P., and Park, K.-S. (2016). Novel Function of Sprouty4 as a Regulator of Stemness and Differentiation of Embryonic Stem Cells. *Dev. Reprod.* **20**, 171–177.
72. Masui, S., Nakatake, Y., Toyooka, Y., Shimosato, D., Yagi, R., Takahashi, K., Okochi, H., Okuda, A., Matoba, R., Sharov, A.A., et al. (2007). Pluripotency governed by Sox2 via regulation of Oct3/4 expression in mouse embryonic stem cells. *Nat. Cell Biol.* **9**, 625–635.
73. Parisi, S., and Russo, T. (2011). Regulatory role of Klf5 in early mouse development and in embryonic stem cells. *Vitam. Horm.* **87**, 381–397.
74. Azami, T., Matsumoto, K., Jeon, H., Waku, T., Muratani, M., Niwa, H., Takahashi, S., and Ema, M. (2018). Klf5 suppresses ERK signaling in mouse pluripotent stem cells. *PLoS One* **13**, e0207321.
75. Godin-Heymann, N., Brabetz, S., Murillo, M.M., Saponaro, M., Santos, C.R., Lobley, A., East, P., Chakravarty, P., Matthews, N., Kelly, G., et al. (2016). Tumour-suppression function of KLF12 through regulation of anoikis. *Oncogene* **35**, 3324–3334.
76. Qi, X., Li, T.-G., Hao, J., Hu, J., Wang, J., Simmons, H., Miura, S., Mischnina, Y., and Zhao, G.-Q. (2004). BMP4 supports self-renewal of embryonic stem cells by inhibiting mitogen-activated protein kinase pathways. *Proc. Natl. Acad. Sci. USA* **101**, 6027–6032.
77. Wu, B., Li, L., Li, B., Gao, J., Chen, Y., Wei, M., Yang, Z., Zhang, B., Li, S., Li, K., et al. (2020). Activin A and BMP4 Signaling Expands Potency of Mouse Embryonic Stem Cells in Serum-Free Media. *Stem Cell Rep.* **14**, 241–255.
78. Estrach, S., Cordes, R., Hozumi, K., Gossler, A., and Watt, F.M. (2008). Role of the Notch ligand Delta1 in embryonic and adult mouse epidermis. *J. Invest. Dermatol.* **128**, 825–832.
79. Nishimura, Y., Kurisaki, A., Nakanishi, M., Ohnuma, K., Ninomiya, N., Komazaki, S., Ishiura, S., and Asashima, M. (2010). Inhibitory Smad proteins promote the differentiation of mouse embryonic stem cells into ciliated cells. *Biochem. Biophys. Res. Commun.* **401**, 1–6.
80. Mulas, C., Kalkan, T., and Smith, A. (2017). NODAL Secures Pluripotency upon Embryonic Stem Cell Progression from the Ground State. *Stem Cell Rep.* **9**, 77–91.

81. Semrau, S., Goldmann, J.E., Soumillon, M., Mikkelsen, T.S., Jaenisch, R., and van Oudenaarden, A. (2017). Dynamics of lineage commitment revealed by single-cell transcriptomics of differentiating embryonic stem cells. *Nat. Commun.* **8**, 1096.
82. Zhao, W., Ji, X., Zhang, F., Li, L., and Ma, L. (2012). Embryonic stem cell markers. *Molecules* **17**, 6196–6236.
83. Trott, J., and Martinez Arias, A. (2013). Single cell lineage analysis of mouse embryonic stem cells at the exit from pluripotency. *Biol. Open* **2**, 1049–1056.
84. Yang, S.-H., Kalkan, T., Morissroe, C., Marks, H., Stunnenberg, H., Smith, A., and Sharrocks, A.D. (2014). Otx2 and Oct4 drive early enhancer activation during embryonic stem cell transition from naive pluripotency. *Cell Rep.* **7**, 1968–1981.
85. Evans, A.L., Faial, T., Gilchrist, M.J., Down, T., Vallier, L., Pedersen, R.A., Wardle, F.C., and Smith, J.C. (2012). Genomic targets of Brachyury (T) in differentiating mouse embryonic stem cells. *PLoS One* **7**, e33346.
86. Navarra, A., Musto, A., Gargiulo, A., Petrosino, G., Pierantoni, G.M., Fusco, A., Russo, T., and Parisi, S. (2016). Hmga2 is necessary for Otx2-dependent exit of embryonic stem cells from the pluripotent ground state. *BMC Biol.* **14**, 24.
87. McFadden, D.G., Barbosa, A.C., Richardson, J.A., Schneider, M.D., Srivastava, D., and Olson, E.N. (2005). The Hand1 and Hand2 transcription factors regulate expansion of the embryonic cardiac ventricles in a gene dosage-dependent manner. *Development* **132**, 189–201. <https://doi.org/10.1242/dev.01562>.
88. Fujiwara, H., Hayashi, Y., Sanzen, N., Kobayashi, R., Weber, C.N., Emoto, T., Futaki, S., Niwa, H., Murray, P., Edgar, D., and Sekiguchi, K. (2007). Regulation of mesodermal differentiation of mouse embryonic stem cells by basement membranes. *J. Biol. Chem.* **282**, 29701–29711.
89. Li, Z., Gadue, P., Chen, K., Jiao, Y., Tuteja, G., Schug, J., Li, W., and Kaestner, K.H. (2012). Foxa2 and H2A.Z mediate nucleosome depletion during embryonic stem cell differentiation. *Cell* **151**, 1608–1616.
90. Niakan, K.K., Ji, H., Maehr, R., Vokes, S.A., Rodolfa, K.T., Sherwood, R.I., Yamaki, M., Dimos, J.T., Chen, A.E., Melton, D.A., et al. (2010). Sox17 promotes differentiation in mouse embryonic stem cells by directly regulating extraembryonic gene expression and indirectly antagonizing self-renewal. *Genes Dev.* **24**, 312–326.
91. Meno, C., Sajoh, Y., Fujii, H., Ikeda, M., Yokoyama, T., Yokoyama, M., Toyoda, Y., and Hamada, H. (1996). Left-right asymmetric expression of the TGF β -family member lefty in mouse embryos. *Nature* **381**, 151–155. <https://doi.org/10.1038/381151a0>.
92. Liu, C., Peng, G., and Jing, N. (2018). TGF- β signaling pathway in early mouse development and embryonic stem cells. *Acta Biochim. Biophys. Sin.* **50**, 68–73.
93. Tripathi, V., Ellis, J.D., Shen, Z., Song, D.Y., Pan, Q., Watt, A.T., Freier, S.M., Bennett, C.F., Sharma, A., Bubulya, P.A., et al. (2010). The nuclear-retained noncoding RNA MALAT1 regulates alternative splicing by modulating SR splicing factor phosphorylation. *Mol. Cell* **39**, 925–938.
94. Ghosh, A., Pandey, S.P., Ansari, A.H., Sundar, J.S., Singh, P., Khan, Y., Ekka, M.K., Chakraborty, D., and Maiti, S. (2022). Alternative splicing modulation mediated by G-quadruplex structures in MALAT1 lncRNA. *Nucleic Acids Res.* **50**, 378–396.
95. Kornblith, A.R., Schor, I.E., Alló, M., Dujardin, G., Petrillo, E., and Muñoz, M.J. (2013). Alternative splicing: a pivotal step between eukaryotic transcription and translation. *Nat. Rev. Mol. Cell Biol.* **14**, 153–165.
96. Kornblith, A.R., de la Mata, M., Fededa, J.P., Munoz, M.J., and Nogues, G. (2004). Multiple links between transcription and splicing. *RNA* **10**, 1489–1498.
97. Naftelberg, S., Schor, I.E., Ast, G., and Kornblith, A.R. (2015). Regulation of alternative splicing through coupling with transcription and chromatin structure. *Annu. Rev. Biochem.* **84**, 165–198.
98. Landeira, D., Sauer, S., Poot, R., Dvorkina, M., Mazzarella, L., Jørgensen, H.F., Pereira, C.F., Leleu, M., Piccolo, F.M., Spivakov, M., et al. (2010). Jarid2 is a PRC2 component in embryonic stem cells required for multi-lineage differentiation and recruitment of PRC1 and RNA Polymerase II to developmental regulators. *Nat. Cell Biol.* **12**, 618–624.
99. Peng, J.C., Valouev, A., Swigut, T., Zhang, J., Zhao, Y., Sidow, A., and Wysocka, J. (2009). Jarid2/Jumonji coordinates control of PRC2 enzymatic activity and target gene occupancy in pluripotent cells. *Cell* **139**, 1290–1302.
100. Olbrich, T., Vega-Sendino, M., Tillo, D., Wu, W., Zolnerowich, N., Pavani, R., Tran, A.D., Domingo, C.N., Franco, M., Markiewicz-Potoczny, M., et al. (2021). CTCF is a barrier for 2C-like reprogramming. *Nat. Commun.* **12**, 4856.
101. Balakrishnan, S.K., Witcher, M., Berggren, T.W., and Emerson, B.M. (2012). Functional and Molecular Characterization of the Role of CTCF in Human Embryonic Stem Cell Biology. *PLoS One* **7**, e42424. <https://doi.org/10.1371/journal.pone.0042424>.
102. Festuccia, N., Owens, N., and Navarro, P. (2018). Esrrb, an estrogen-related receptor involved in early development, pluripotency, and reprogramming. *FEBS Lett.* **592**, 852–877. <https://doi.org/10.1002/1873-3468.12826>.
103. Latos, P.A., Goncalves, A., Oxley, D., Mohammed, H., Turro, E., and Hemberger, M. (2015). Fgf and Esrrb integrate epigenetic and transcriptional networks that regulate self-renewal of trophoblast stem cells. *Nat. Commun.* **6**, 7776. <https://doi.org/10.1038/ncomms8776>.
104. Kidder, B.L., and Palmer, S. (2012). HDAC1 regulates pluripotency and lineage specific transcriptional networks in embryonic and trophoblast stem cells. *Nucleic Acids Res.* **40**, 2925–2939.
105. Jamalladin, S., Kelly, R.D.W., O'Regan, L., Dovey, O.M., Hodson, G.E., Millard, C.J., Portolano, N., Fry, A.M., Schwabe, J.W.R., and Cowley, S.M. (2014). Histone deacetylase (HDAC) 1 and 2 are essential for accurate cell division and the pluripotency of embryonic stem cells. *Proc. Natl. Acad. Sci. USA* **111**, 9840–9845.
106. Dahlet, T., Argüeso Lleida, A., Al Adhami, H., Dumas, M., Bender, A., Ngondo, R.P., Tanguy, M., Vallet, J., Auclair, G., Bardet, A.F., and Weber, M. (2020). Genome-wide analysis in the mouse embryo reveals the importance of DNA methylation for transcription integrity. *Nat. Commun.* **11**, 3153.
107. Gu, T., Lin, X., Cullen, S.M., Luo, M., Jeong, M., Estecio, M., Shen, J., Hardikar, S., Sun, D., Su, J., et al. (2018). DNMT3A and TET1 cooperate to regulate promoter epigenetic landscapes in mouse embryonic stem cells. *Genome Biol.* **19**, 88.
108. Das, S., and Krainer, A.R. (2014). Emerging functions of SRSF1, splicing factor and oncoprotein, in RNA metabolism and cancer. *Mol. Cancer Res.* **12**, 1195–1204.
109. Gonçalves, V., and Jordan, P. (2015). Posttranscriptional Regulation of Splicing Factor SRSF1 and Its Role in Cancer Cell Biology. *BioMed Res. Int.* **2015**, 287048.
110. Maslon, M.M., Heras, S.R., Bellora, N., Eyras, E., and Cáceres, J.F. (2014). The translational landscape of the splicing factor SRSF1 and its role in mitosis. *Elife* **3**, e02028.
111. Haward, F., Maslon, M.M., Yeyati, P.L., Bellora, N., Hansen, J.N., Aitken, S., Lawson, J., von Kriegsheim, A., Wachtjen, D., Mill, P., et al. (2021). Nucleo-cytoplasmic shuttling of splicing factor SRSF1 is required for development and cilia function. *Elife* **10**, e65104. <https://doi.org/10.7554/eLife.65104>.
112. Liu, Y., Luo, Y., Shen, L., Guo, R., Zhan, Z., Yuan, N., Sha, R., Qian, W., Wang, Z., Xie, Z., et al. (2020). Splicing Factor SRSF1 Is Essential for Satellite Cell Proliferation and Postnatal Maturation of Neuromuscular Junctions in Mice. *Stem Cell Rep.* **15**, 941–954.
113. Xu, Y., Zhao, W., Olson, S.D., Prabhakara, K.S., and Zhou, X. (2018). Alternative splicing links histone modifications to stem cell fate decision. *Genome Biol.* **19**, 133.

114. Ding, F., Su, C.J., Edmonds, K.K., Liang, G., and Elowitz, M.B. (2022). Dynamics and functional roles of splicing factor autoregulation. *Cell Rep.* 39, 110985.
115. Theka, I., Sottile, F., Cammisa, M., Bonnin, S., Sanchez-Delgado, M., Di Vicino, U., Neguembor, M.V., Arumugam, K., Aulicino, F., Monk, D., et al. (2019). Wnt/β-catenin signaling pathway safeguards epigenetic stability and homeostasis of mouse embryonic stem cells. *Sci. Rep.* 9, 948.
116. Huang, G.-W., Zhang, Y.-L., Liao, L.-D., Li, E.-M., and Xu, L.-Y. (2017). Natural antisense transcript TPM1-AS regulates the alternative splicing of tropomyosin I through an interaction with RNA-binding motif protein 4. *Int. J. Biochem. Cell Biol.* 90, 59–67.
117. Duan, Y., Jia, Y., Wang, J., Liu, T., Cheng, Z., Sang, M., Lv, W., Qin, J., and Liu, L. (2021). Long noncoding RNA DGCR5 involves in tumorigenesis of esophageal squamous cell carcinoma via SRSF1-mediated alternative splicing of Mcl-1. *Cell Death Dis.* 12, 587.
118. He, R.-Z., Luo, D.-X., and Mo, Y.-Y. (2019). Emerging roles of lncRNAs in the post-transcriptional regulation in cancer. *Genes Dis.* 6, 6–15.
119. Malgowska, M., Czajczynska, K., Gudanis, D., Tworak, A., and Gdaniec, Z. (2016). Overview of the RNA G-quadruplex structures. *Acta Biochim. Pol.* 63, 609–621.
120. Szabat, M., Kierzek, E., and Kierzek, R. (2018). Modified RNA tripleplexes: Thermodynamics, structure and biological potential. *Sci. Rep.* 8, 13023.
121. Rakheja, I., Ansari, A.H., Ray, A., Chandra Joshi, D., and Maiti, S. (2022). Small molecule quercetin binds triplex and modulates its cellular function. *Mol. Ther. Nucleic Acids* 30, 241–256.
122. Xu, S., Lai, S.-K., Sim, D.Y., Ang, W.S.L., Li, H.Y., and Roca, X. (2022). SRPM2 organizes splicing condensates to regulate alternative splicing. *Nucleic Acids Res.* 50, 8599–8614.
123. Hime, G., and Abud, H. (2013). *Transcriptional and Translational Regulation of Stem Cells* (Springer Science & Business Media).
124. Kim, S.K., Selleri, L., Lee, J.S., Zhang, A.Y., Gu, X., Jacobs, Y., and Cleary, M.L. (2002). Pbx1 inactivation disrupts pancreas development and in *Lpf1*-deficient mice promotes diabetes mellitus. *Nat. Genet.* 30, 430–435.
125. Linares, A.J., Lin, C.-H., Damianov, A., Adams, K.L., Novitch, B.G., and Black, D.L. (2015). The splicing regulator PTBP1 controls the activity of the transcription factor Pbx1 during neuronal differentiation. *Elife* 4, e09268.
126. Curado, J., Iannone, C., Tilgner, H., Valcárcel, J., and Guigó, R. (2015). Promoter-like epigenetic signatures in exons displaying cell type-specific splicing. *Genome Biol.* 16, 236.
127. Kelstrup, C.D., Jersie-Christensen, R.R., Batth, T.S., Arrey, T.N., Kuehn, A., Kellmann, M., and Olsen, J.V. (2014). Rapid and deep proteomes by faster sequencing on a benchtop quadrupole ultra-high-field Orbitrap mass spectrometer. *J. Proteome Res.* 13, 6187–6195.
128. Cox, J., and Mann, M. (2008). MaxQuant enables high peptide identification rates, individualized p.p.b.-range mass accuracies and proteome-wide protein quantification. *Nat. Biotechnol.* 26, 1367–1372.
129. Concordet, J.-P., and Haeussler, M. (2018). CRISPOR: intuitive guide selection for CRISPR/Cas9 genome editing experiments and screens. *Nucleic Acids Res.* 46, W242–W245.
130. Ran, F.A., Hsu, P.D., Wright, J., Agarwala, V., Scott, D.A., and Zhang, F. (2013). Genome engineering using the CRISPR-Cas9 system. *Nat. Protoc.* 8, 2281–2308.
131. Livak, K.J., and Schmittgen, T.D. (2001). Analysis of relative gene expression data using real-time quantitative PCR and the 2-(Delta Delta CT) Method. *Methods* 25, 402–408.

STAR★METHODS

KEY RESOURCES TABLE

REAGENT or RESOURCE	SOURCE	IDENTIFIER
Antibodies		
anti-eGFP	Abcam	ab920
anti-HA	Abcam	ab9110; RRID:AB_307019
anti-Cxorf23 (TOBF1)	Abcam	ab179446
anti-PAX6	Abcam	ab5790; RRID:AB_305110
anti-Gata6	Abcam	ab22600
anti-Ncadherin	Thermo	33–3900
anti-RPS26	Abcam	ab229571
anti-SON	Abcam	ab121759
anti-SC35 (SRSF2)	Abcam	ab11826; RRID:AB_298608
anti-SRSF1 (SF2)	Abcam	ab133869
Anti-Beta Tubulin (Loading control)	Abcam	ab6046; RRID:AB_2210370
Alexa Flour labeled secondary antibodies	Invitrogen	N/A
Bacterial and virus strains		
DH5 alpha	Lab of Dr. Debojyoti Chakraborty	N/A
Chemicals, peptides, and recombinant proteins		
Demecolcine	Sigma Aldrich	D1925
Recombinant Leukemia Inhibitory Factor	MPI-CBG	NA
Propidium Iodide	Sigma Aldrich	P4170
Critical commercial assays		
PrimeScript 1 st strand cDNA synthesis kit	TaKaRa	6110A
TB Green® Premix Ex Taq™ II (Tli RNase H Plus)	TaKaRa	RR82LR
Deposited data		
Raw and analyzed data of RNA Sequencing	This paper	SRA database (PRJNA900687)
Raw and analyzed data of Proteomics	This paper	PRIDE (PXD044905)
Experimental models: Cell lines		
Mouse ES cells (R1/E)	Gift from Dr. Frank Buchholz lab	N/A
N2A and B16 cell line	Gift from Dr. Beena Pillai lab	N/A
Mouse Tissues	Gift from Dr. Beena Pillai lab	N/A
MEF cell line	Gift from Dr. Shravanti Ramapalli lab	N/A
Oligonucleotides		
Primers (see Table S9)	This paper	N/A
Recombinant DNA		
pCaggs-3XHA TOBF1	Lab of Dr. Debojyoti Chakraborty	N/A
Px458-dual sgRNA	Px458 (#48138) was a gift from Feng Zhang lab. Px333 was a gift from Andrea Ventura. Bsal sgRNA scaffold was taken from Px333 (#64073) and subcloned in Px458 to create the Px458- dual sgRNA vector	RRID:Addgene_48138, RRID:Addgene_64073

(Continued on next page)

Continued

REAGENT or RESOURCE	SOURCE	IDENTIFIER
dFnCas9-KRAB	dSpCas9-KRAB mcherry (#60954) was a gift from Jonathan Weissman. KRAB sequence was taken from dSpCas9-KRAB-mcherry vector and cloned in Px458-FnCas9 (#130969) vector prepared in Lab of Dr. Debojyoti Chakraborty	RRID:Addgene_60954, RRID:Addgene_130969
Software and algorithms		
Fiji	ImageJ	https://imagej.net/software/fiji/
SUPPA2	NA	https://genomebiology.biomedcentral.com/articles/10.1186/s13059-018-1417-1
RSEM-STAR	NA	https://deweylab.github.io/RSEM/README.html
EdgeR	NA	https://www.ncbi.nlm.nih.gov/pmc/articles/PMC2796818/
GraphPad Prism 8.4	GraphPad	https://www.graphpad.com
FlowJo ver 10.6	FlowJo	https://www.flowjo.com

RESOURCE AVAILABILITY

Lead contact

Resources and reagent requests should be directed to the lead contact, Dr. Debojyoti Chakraborty (debojyoti.chakraborty@igib.in)

Materials availability

The study did not generate new unique reagents.

Data and code availability

- RNA-Seq data and Proteomics data have been deposited at Sequence Read Archive (SRA) data based and PRIDE repository, respectively and are publicly available as of the date of publication. Accession numbers are listed in the [key resources table](#)
- This paper does not report original code.
- Any additional information required to reanalyze the data reported in this work paper is available from the [lead contact](#) upon request.

EXPERIMENTAL MODEL AND STUDY PARTICIPANT DETAILS

Cell lines and cell culture

Mouse embryonic stem cell culture

Mouse embryonic stem cell line, R1/E cultured in feeder-free complete media containing 1X DMEM (Gibco, 11995-065), 20% Fetal Bovine Serum (Pansera Pan Biotech, P29-0705-ES), 1X Pen-strep (Gibco, 15140122), 1% NEAA (Gibco, 11140050), 0.1% Beta-Mercaptoethanol (Gibco, 21985023) with additional supplement of 8 ng/ml LIF (MPI-CBG, Dresden, Germany) per 500mL of media. The mESCs were cultured up to a maximum of 20 passages. Media were changed every day and split every alternate day by detaching with 0.25% Trypsin-EDTA (Gibco, 25200056). Cells were incubated in a humified incubator at 37°C and 5% CO₂.

Other cell line culture

Mouse neuroblast cell line, N2A, mouse melanoma cell line, B16, Mouse Embryonic Fibroblast cell line, MEF cell lines were cultured in 1X DMEM, high glucose, GlutaMAX supplement (Gibco, 10569010) with 10% Fetal bovine serum (Gibco, 16000044) with 1X Antibiotic-Antimycotic (15240062). Cell were incubated in a humified incubator at 37°C and 5% CO₂.

METHOD DETAILS

Cells transfection and harvesting

Cells were seeded in 6 well or 12 well plates with 8×10^4 or 4×10^4 seeding density respectively. 16-20hrs post seeding, cells were transfected with 2ug per well (6 well plate) and 1ug per well (12 well plate) of plasmids concentration with the transfection reagent Lipofectamine 3000 (Invitrogen, L3000001) and the protocol mentioned in the kit was followed. 48-72hrs post transfection, cells were harvested for downstream experiment.

Cells synchronization

For synchronizing ES cells in M phase, following trypsinization cells were washed in 1x PBS and released in fresh media containing 20 ng/mL Demecolcine (SigmaAldrich, D1925). After an incubation at 37°C and 5% CO₂ for 4h, cells were further washed twice with 1x PBS, released into Demecolcine-free media for 2h for entry into G1 and subsequently trypsinized and collected for further studies.

Affinity pull-down and mass spectrometry

G1 synchronized cells were washed with ice-cold 1XPBS 2 or 3 times. These cells were then lysed with cell lysis RIPA buffer (7.5 pH 50mM Tris, 1% NP-40 (nonyl phenoxy polyethoxylethanol), 0.1% Na-deoxycholate, 1mM EDTA, Protease Inhibitors cocktail (PIC), 100-150mM NaCl). Cells are incubated with lysis buffer for about 5 min on ice. Cell lysates are collected by centrifuging at 13K rpm for 15-20 mins at 4°C. After the spin, supernatant was taken in a separate tube by filtering with 45um filter to remove lipids.

For pull down with anti-GFP antibody, 20ul of Chromtek anti-GFP trap magnetic bead slurry taken (washed with 1xPBS once) and then added to cell lysate. This lysate mixed with anti-GFP beads were incubated by rotating at 4°C for 2-4hrs. Post incubation, beads were washed with RIPA+ 1XPIC twice and followed by wash with water four times to remove detergents and salts to avoid interference with MS analysis. After wash, we tried to remove as much liquid as possible and 150uL of 8M GuHCl added to the beads for elution.

The lysate was used as input material for affinity enrichment with magnetic beads precoupled to anti-GFP antibodies followed by trypsin digestion. The tryptic digest was desalted and analyzed on an EASY-nLC system (Thermo Scientific) connected to a Q-Exactive (Thermo Scientific) mass spectrometer.¹²⁷ Maxquant software was used to analyze raw mass spectrometry data files.¹²⁸ The data was filtered using the target-decoy strategy to allow a maximum of 1% false identification both on the peptide and protein levels.

Generating TOBF1 KO cells

crRNAs targeting Exon 2, 3 and 4 (ChX: 59548256:159548275, 159551902:159551921, 159552068:159552087, 159553459: 159553478) of Tobf1 gene were designed with CRISPOR tool.¹²⁹ These crRNAs were cloned in SpCas9 with GFP reporter (Dual sgRNA Px458) vector which has scaffold for dual sgRNA cloning. This vector was designed for visualization and fluorescent based cell sorting. 4 crRNAs were designed and cloned using BbsI restriction enzyme based cloning strategy in 2 vectors using the protocol for sgRNA cloning¹³⁰ and confirmed with sanger sequencing. Oligo sequences of the crRNA forming DNA template and vector maps have been provided in the Table S9. These two vectors were pooled and transfected with Lipofectamine3000 using the protocol provided in the kit. 48hrs post transfection, cells were harvested and single cells and bulk cells sorted based on GFP expression with BD FACS Melody cell sorter which uses the BD FACS Chorus software. Cells are seeded in the same complete media and KO cells are confirmed with qPCR and Western Blot in the subsequent passages.

Over-expression of TOBF1

Total mESCs RNA was used to synthesize total cDNA with Superscript III First strand synthesis kit (Invitrogen, 18080051). The full-length Tobf1 cDNA sequence (~2.3 kb) (UCSC ENSMUST00000112464.8 chrX:158331271–158375174) was then synthesized from the total cDNA by using Tobf1 specific cDNA Agel containing forward and Xhol containing reverse primers which is listed in Table S9. The PCR was done by using Q5 High-fidelity DNA Polymerase (New England Biolabs, M0491) in a mix carrying 10 μL Q5 PCR buffer (5x), 2.5 μL 10 μM primers, 1ul 10mM dNTP mix (Invitrogen) and 5ul of total mESCs cDNA. The volume was adjusted to 50 μL using PCR grade water. The reaction was set up in a DNA Thermocycler (Bio-Rad) and the conditions for PCR were: Initial denaturation at 98°C for 2 min followed by 40 cycles of denaturation, annealing and extension (98°C for 10 s, 65°C for 45 s, 72°C for 3 min) and a final extension at 72°C for 10 min.

The PCR amplicons were purified using a PCR purification kit (Qiagen). This PCR amplicon was fused with Kozak 3XHA (~100 bps) amplified product by using overlapping primers having NheI forward and Xhol containing primers and the PCR was conducted using the same protocol mentioned above. This 3XHA Tobf1 CDS product (~2.4 kb) was digested with NheI and Xhol restriction enzymes and ligated into the vector pCAGGS-RFP in which the RFP sequence was replaced with the PCR product. Successful cloning was confirmed by Sanger Sequencing.

RNA extraction methods

For extracting cells in the G1 phase, ES FUCCI vector was transfected in TOBF1 KO, OE and Control cells and as G1 phase is indicated by the expression of reporter gene mCherry, we FACS sorted cells expressing either mCherry (G1) or non-mCherry (non G1) cells and examined the steady state levels of Tobf1 in these two sorted populations. For RNA isolation, TOBF1 over-expressed and knock-out samples along with controls are sequenced in three independent biological replicates on Illumina Hi-Seq platform.

RNA sequencing analysis

Quality control for all samples was assessed using FastQC. Low-quality reads and adaptor contamination were removed through Trimmomatic. The RSEM reference index was generated using mouse reference genome (GRCm39/mm39) and transcriptome (gencode.vM27) with the rsem-prepare-reference command coupled with STAR aligner. Subsequently, Gene expressions were estimated by alignment of sequencing reads to the reference index with STAR and rsem-calculate-expression command. Further, gene

count matrix was generated with test and control samples for both the knockout and over-expression of *Tobf1*. Gene expression counts were normalized using TMM followed by differential expression using generalized linear model quasi-likelihood F-tests (glmQLFTest) from the edgeR Bioconductor package. Top differentially expressed genes were visualized with the help of the EnhancedVolcano Bioconductor package. The Complex Heatmap package from Bioconductor was used to generate heatmap.

For estimating the splicing events, a pipeline, as described in the SUPPA2 package, was executed. As recommended in the SUPPA2 tutorial, reference indexes were built from mouse transcriptome (gencode.vM27) followed by the pseudo alignment of the reads to generate transcript counts using salmon aligner. Further, reference for various splicing events is built from gencode.vM27 using ‘generateEvents’ sub-command of SUPPA2. Transcript quantification files from the salmon aligner were used to generate a matrix followed by the estimation of local alternative splicing events with ‘psiPerEvent’ sub-command of SUPPA2. Differential splicing events were calculated by diffSplice SUPPA2 sub-command with the empirical method. Any splicing events with a difference of greater than $|0.10|$ PSI were considered statistically significant. Splicing events between different conditions are visualized using sashimi plots with ggsashimi tool. Gene expression, splicing and ChIP-Seq data is integrated and visualized through the Circilize package.

For pathway and gene enrichment analysis, clusterProfiler has been fed with differential expressed transcripts to predict the gene ontology and wiki pathways. This process is also performed for genes with differential splicing events as well as for proteomics data from mass-spectroscopy.

qRT-PCR

Total RNA was isolated from mES cells 48 h post transfection. Qiagen RNeasy kit (74106) was used to isolate total RNA in the stepwise protocol provided with the kit. The RNA isolated was treated with DNaseI (Turbo DNase kit, Invitrogen, AM2238). cDNA synthesis was done from DNaseI treated total RNA with Qiagen cDNA synthesis kit (205313) with the incubation conditions suggested with the kit. cDNA synthesis was followed by real time qPCR for the test and control samples in triplicates. The transcripts were quantified by using SYBR Green Master Mix: SYBR green based TB Green Premium Ex Taq II (Takara, RR82WR) in the PCR instrument Light Cycler 480 (Roche) or BioRad. All the C_t values obtained for different transcripts were normalized with the C_t value of Beta-Actin. The Fold change analysis of the transcripts for comparative analysis was done using the $2^{-\Delta\Delta C_t}$ method.¹³¹

Western blot

The ES cells were lysed using RIPA lysis buffer (ThermoFisher, Pierce) to prepare the cell protein lysate. 100 μ L of the lysis buffer was added to each 6-well plate along with 1× Protease Inhibitor Cocktail (PIC, Roche cComplete). The cells were incubated in a rocker at 4°C for 1hr. Protein lysate from each sample was collected and the concentration of the protein was estimated using Pierce BCA Protein Assay Kit (ThermoFisher). For each sample, 30 μ g of protein was loaded into the wells of 10% SDS gel and PAGE was performed using SDS running buffer (2.5mM Tris base, 19mM Glycine, 0.1% SDS in autoclaved milliQ). The proteins were then transferred from the gel to the PVDF membrane (GE Healthcare Life-Science) in Bio-Rad vertical gel Transfer Apparatus using Transfer buffer (2.5mM Tris base, 19mM Glycine, 20% v/v Methanol in autoclaved milliQ) at 4°C for 1.5 h at 95 V. After the transfer was complete, the membrane was cut according to the required protein size and kept for blocking with 5% BSA in 1×TBST (20mM Tris base, 150 mM NaCl and 0.2% Tween 20) on a rocker at room temperature for 2 h. After blocking, the blots were incubated with primary antibody at 1:1000 dilution in the same blocking buffer overnight in a rocker at 4°C. Beta-Tubulin antibody (1:5000 dilution) is taken as the loading control. After primary antibody incubation, the blots were washed three times for 10 min each with 0.2% TBST. Post washing, the same blots were incubated with a secondary antibody having HRP conjugate in a rocker for 2 h at room temperature. Post secondary antibody incubation, the blots were washed three times for 15 min each. For signal development, EMD Millipore Immobilon Western Chemiluminescent HRP Substrate (ECL) was used to develop the blots in the Syngene Gel doc instrument. ImageJ was used for the densitometry analysis and quantification of the signals.

Immunofluorescence (IF)

For slide preparation, R1E mES cells or TOBF1 GFP cells were seeded in 0.1% Gelatin pre-coated 22 × 22mm coverslips (Corning, CLS285022) placed in a 6 well plate. ~8×10⁴ cells seeded and 24hrs post seeding and adherence, cells were harvested by washing with 1×PBS (Gibco, 10010023) twice in a well plate. All the procedure since harvesting was carried out in the well plates that contained the cell adhered coverslips. Cells were then fixed with chilled 4% Paraformaldehyde (PFA) + EDTA (Ph 7.4) by incubating at Room Temperature (RT) for 10 min in a mild shaker. Post fixation, the coverslips were washed twice with a washing buffer (10 μ M MgCl₂, 5 μ M EGTA in 1×PBS). Cells were then incubated with a permeabilization buffer (0.2% Triton X-100, 10 μ M MgCl₂, 5 μ M EGTA in 1×PBS) at RT for 10 min followed by washing with a washing buffer twice. After permeabilization, cells were incubated with blocking buffer (2% BSA, 10 μ M MgCl₂, 5 μ M EGTA in 1×PBS) for 15 min at 37°C. After blocking, the cells were incubated with primary antibodies in the ratio of 1:250 dilution in the same blocking buffer. Incubation was done for 2 hrs at 37°C or overnight at 4°C. For Co-IF studies, two antibodies raised in different species were mixed in 1:250 dilution ratio in blocking buffer and incubated in the same manner post fixation and permeabilization of the cells in coverslips. Once the primary incubation time was completed, the cells were washed with 1×PBS thrice for 5mins each. Now the cells were incubated with Alexa fluor labeled fluorescent secondary antibodies (ThermoFisher Scientific) to be conjugated specifically with the primary antibody, considering the species in which it is raised. Fluorescently tagged secondary antibodies were used in the dilution ratio of 1:1000 in the same blocking buffer and incubated

for 30 min at RT. Post incubation, the cells are washed with 1×PBS thrice for 5mins each. After the wash, one drop of ProLong Diamond Antifade mountant with DAPI (Invitrogen, P369366) was added in each coverslip and these coverslips were then mounted on one side frosted glass slides (Corning, CLS294875X25) and proceeded for imaging. For colocalization, DeltaVision Ultra-light microscope (GE Healthcare) was used for imaging the slides at 60× objective with the help of DV SoftWorx software. iT2 confocal microscope (Nikon) was used for imaging differentiation experiments at 60× objective (2X zoom), NIS elements software used for post-acquisition processing. Mean intensities were quantified by ImageJ tool. Co-localization quantification studies of all images were done in ImageJ with Coloc2 and JACoP plugins by determining the Pearson's and Mander's coefficients.

Immunoprecipitation (IP)

1×10^6 cells were seeded in a 100mm dish (Corning) and 16hrs post seeding appropriate transfection was done according to desired experiment. 48hrs post transfection, cells were washed and trypsinized and cross-linked with 1% Formaldehyde by incubating at RT for 15mins. Formaldehyde was quenched by adding 125mM Glycine to the formaldehyde and incubated at RT for 10mins. Pellet down the cells by centrifuging at 1200 rpm for 5mins. The cell pellet was washed twice and lyse the cells with RIPA cell lysis and extraction buffer (Thermo Scientific, 89900) and 1x Protease Inhibitor cocktail (PIC) (Roche, SKU11697498001). The total protein concentration in the cell lysate was quantified by using BCA protein Assay kit (Thermo Scientific, 23225). For pre-clearing of lysate: Equal concentration of lysate taken for test and control samples and these lysates were pre-cleared with 5ug of IgG isotype control (ab171870) and 15ul of 30 mg/ml Dynabeads protein A (Invitrogen, 10001D) at 4°C for 2hrs on a rotator. Following that we proceeded with beads blocking. In separate vials, 35ul of Dynabeads Protein A is taken for each sample for immunoprecipitation and these beads are once washed with 1×PBS and then allowed to incubate with 2% BSA and 10 ng/ml Yeast tRNA (Thermo Scientific, AM7119) for blocking the beads to avoid non-specific binding of proteins and RNAs. This incubation is done at 4°C for 2hrs on a rotator. Antibody binding with blocked beads: Blocked Beads are incubated with 5-10 μ g of ChIP grade anti-HA antibody (ab9110) in 1×PBS and allowed to incubate at 4°C for 4hrs on a rotator. Lysate and beads binding: Beads from Pre-cleared lysate is removed by placing it in a magnetic stand and this pre-cleared lysate is then allowed to incubate with the antibody bound beads 4°C for 12-16hrs (O/N) on a rotator. A small volume of each sample is kept aside as 1–5% input which is not subjected to antibody binding and pull-down. After incubation completion, the beads samples were washed with RIPA buffer thrice and then the beads were incubated with Elution buffer (1%SDS, 10mM NaHCO₃) at 30°C for 30mins. The eluted samples were checked with Western blot along with 1% input sample.

Cell cycle assay

The cells were harvested by trypsinizing them and washing them with cold 1×PBS. This was spinned at 1500xg for 5 min. The pellet was fixed with chilled 70% Ethanol in a dropwise manner, while gently vortexing the pellet. This was again spinned at 1500 xg for 5 min. The pellet was resuspended with a buffer (0.1% Triton X-+RNaseA in1xPBS) and incubated at 37°C for 3 h. Post incubation, Propidium Iodide (PI) (5ug/ml) was added to all the samples required for acquisition. For acquisition of the samples, BD LSR II FACS system was used and analysis of different cell cycle was done using FlowJo v10.6 software.

QUANTIFICATION AND STATISTICAL ANALYSIS

The statistical analysis for experiments was performed using GraphPad Prism 8.4 to evaluate significance among experimental replicates. All data were presented as mean \pm S.D. of three independent biological replicates except otherwise mentioned. A two-tailed unpaired Student's t-test was used to analyze the qRT-PCR and WB experimental data. The experimental results leading to a p-value < 0.05 were considered statistically significant. One asterisk (*), two asterisks (**), three asterisks (***) denote p < 0.05, p < 0.001 and p < 0.0001, respectively.